2

Ring Resonators: Theory and Modeling

One of the first papers dealing with the simulation of an integrated ring resonator for a bandpass filter has been published in 1969 by Marcatili. The layout of the channel dropping filter which he proposed is shown in Fig. 2.1. This can be regarded as the standard configuration for an integrated ring resonator channel dropping filter. Two straight waveguides also known as the bus or the port waveguides are coupled either by directional couplers through the evanescent field or by multimode interference (MMI) couplers to the ring resonator. A simpler configuration is obtained, when the second bus or port waveguide is removed. Then the filter is typically referred to as "notch" filter because of the unique filter characteristic. In the following chapter, the ring resonator simulation model is described beginning with the basic notch configuration and adding more bus waveguides and ring resonators to eventually build a multiple coupled ring resonator filter. Different types of ring resonator simulation models will be explained, so as to be able to chose from a range of models which best suit the need.

2.1 Single Ring Resonators

2.1.1 Ring Structure

The Basic Configuration

The basic configuration, which consists of unidirectional coupling between a ring resonator with radius r and a waveguide, is described in Fig. 2.2, based on Yariv (2002a, b). Defining that a single unidirectional mode of the resonator is excited, the coupling is lossless, single polarization is considered, none of the waveguide segments and coupler elements couple waves of different polarization, the various kinds of losses occurring along the propagation of

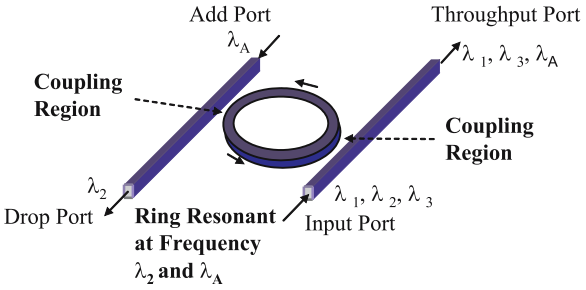

Fig. 2.1. Ring resonator channel dropping filter

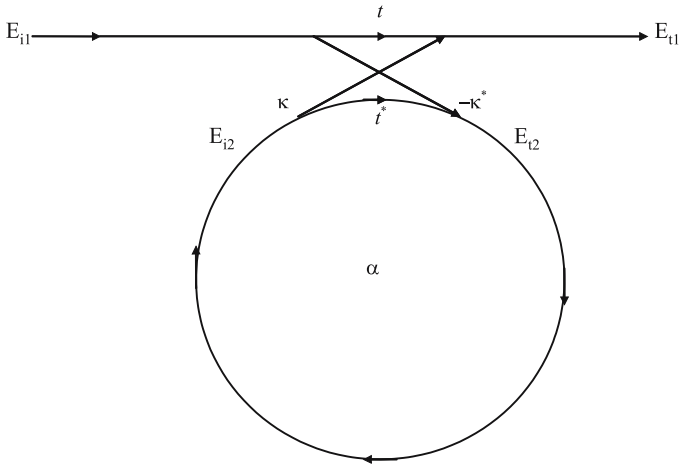

Fig. 2.2. Model of a single ring resonator with one waveguide

light in the ring resonator filter are incorporated in the attenuation constant, the interaction can be described by the matrix relation:

$$\begin{pmatrix} E_{t1} \\ E_{t2} \end{pmatrix} = \begin{pmatrix} t & \kappa \\ -\kappa^* & t^* \end{pmatrix} \begin{pmatrix} E_{i1} \\ E_{i2} \end{pmatrix}. \tag{2.1}$$

The complex mode amplitudes E are normalized, so that their squared magnitude corresponds to the modal power. The coupler parameters t and κ depend on the specific coupling mechanism used. The * denotes the conjugated complex value of t and κ, respectively.

The matrix is symmetric because the networks under consideration are reciprocal. Therefore

$$\left|\kappa^2\right| + \left|t^2\right| = 1. \tag{2.2}$$

In order to further simplify the model, E_{i1} is chosen to be equal to 1. Then the round trip in the ring is given by

$$E_{i2} = \alpha \cdot \mathrm{e}^{\mathrm{j}\theta} E_{t2}, \tag{2.3}$$

where α is the loss coefficient of the ring (zero loss: $\alpha = 1$) and $\theta = \omega L/c$, L being the circumference of the ring which is given by $L = 2\pi r$, r being the radius of the ring measured from the center of the ring to the center of the waveguide, c the phase velocity of the ring mode ($c = c_0/n_{\text{eff}}$) and the fixed angular frequency $\omega = kc_0$, c_0 refers to the vacuum speed of light. The vacuum wavenumber k is related to the wavelength λ through: $k = 2\pi/\lambda$. Using the vacuum wavenumber, the effective refractive index n_{eff} can be introduced easily into the ring coupling relations by

$$\beta = k \cdot n_{\text{eff}} = \frac{2\pi \cdot n_{\text{eff}}}{\lambda}, \tag{2.4}$$

where β is the propagation constant. This leads to

$$\theta = \frac{\omega L}{c} = \frac{kc_0 L}{c} = k \cdot n_{\text{eff}} \cdot 2\pi r = \frac{2\pi \cdot n_{\text{eff}} \cdot 2\pi r}{\lambda} = 4\pi^2 n_{\text{eff}} \frac{r}{\lambda}. \tag{2.5}$$

From (2.1) and (2.3) we obtain

$$E_{t1} = \frac{-\alpha + t \cdot \mathrm{e}^{-\mathrm{j}\theta}}{-\alpha t^* + \mathrm{e}^{-\mathrm{j}\theta}}, \tag{2.6}$$

$$E_{i2} = \frac{-\alpha\kappa^*}{-\alpha t^* + \mathrm{e}^{-\mathrm{j}\theta}}, \tag{2.7}$$

$$E_{t2} = \frac{-\kappa^*}{1 - \alpha t^* \mathrm{e}^{\mathrm{j}\theta}}. \tag{2.8}$$

This leads to the transmission power P_{t1} in the output waveguide, which is

$$P_{t1} = |E_{t1}|^2 = \frac{\alpha^2 + |t|^2 - 2\alpha\,|t| \cos(\theta + \varphi_{\text{t}})}{1 + \alpha^2\,|t|^2 - 2\alpha\,|t| \cos(\theta + \varphi_{\text{t}})}, \tag{2.9}$$

where $t = |t| \exp(\mathrm{j}\varphi_{\text{t}})$, $|t|$ representing the coupling losses and φ_t the phase of the coupler.

The circulating power P_{i2} in the ring is given by

$$P_{i2} = |E_{i2}|^2 = \frac{\alpha^2(1 - |t|^2)}{1 + \alpha^2\,|t|^2 - 2\alpha\,|t| \cos(\theta + \varphi_{\text{t}})}. \tag{2.10}$$

On resonance, $(\theta + \varphi_t) = 2\pi m$, where m is an integer, the following is obtained:

$$P_{t1} = |E_{t1}|^2 = \frac{(\alpha - |t|)^2}{(1 - \alpha\,|t|)^2} \tag{2.11}$$

and

$$P_{i2} = |E_{i2}|^2 = \frac{\alpha^2(1 - |t|^2)}{(1 - \alpha\,|t|)^2}. \tag{2.12}$$

A special case happens when $\alpha = |t|$ in (2.11), when the internal losses are equal to the coupling losses. The transmitted power becomes 0. This is known in literature as critical coupling, which is due to destructive interference.

In using the above equations, it is possible to get a good idea of the behavior of a simplified basic ring resonator filter configuration consisting of only one waveguide and one ring. The wavelength-dependent filter characteristic for a ring resonator configuration with a radius of $r = 148\,\mu\text{m}$ with matched coupling and loss coefficient, derived using (2.1)–(2.11), is shown in Fig. 2.3. This model can be extended to suit the requirement of various types of ring resonator configurations.

The next configuration which is discussed is the basic ring resonator add–drop configuration, consisting of one input, one output waveguide and the ring resonator. The four ports of the ring resonator are referred to in the following as input port, throughput port, drop port and add port (Fig. 2.4).

The ring resonator simulation model has been updated according to Fig. 2.4. For simplification E_{i1} is as defined before equal to 1. The throughput mode amplitude in the first waveguide is given by

$$E_{t1} = t_1 + \frac{-\kappa_1\kappa_1^* t_2^* \alpha_{1/2}^2 \mathrm{e}^{\mathrm{j}\theta|t_1|^2+|\kappa_1|^2=1}}{1 - t_1^* t_2^* \alpha_{1/2}^2 \mathrm{e}^{\mathrm{j}\theta}} = \frac{t_1 - t_2^* \alpha_{1/2}^2 \mathrm{e}^{\mathrm{j}\theta}}{1 - t_1^* t_2^* \alpha_{1/2}^2 \mathrm{e}^{\mathrm{j}\theta}} = \frac{t_1 - t_2^* \alpha \mathrm{e}^{\mathrm{j}\theta}}{1 - t_1^* t_2^* \alpha \mathrm{e}^{\mathrm{j}\theta}}. \tag{2.13}$$

In this calculation, $\alpha_{1/2}$ and $\theta_{1/2}$ are used which are the half round trip loss and phase, respectively. It is $\alpha = \alpha_{1/2}^2$ and $\theta = 2\theta_{1/2}$.

Now, the mode amplitude in the ring has to pass the second coupler as can be seen from the schematic to become the new dropped mode amplitude E_{t2}. The dropped mode amplitude in the second waveguide is then given by:

$$E_{t2} = \frac{-\kappa_1^* \kappa_2 \alpha_{1/2} \mathrm{e}^{\mathrm{j}\theta_{1/2}}}{1 - t_1^* t_2^* \alpha \mathrm{e}^{\mathrm{j}\theta}}. \tag{2.14}$$

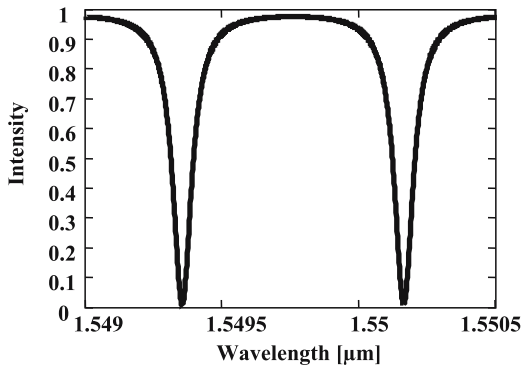

Fig. 2.3. Notch type ring resonator filter characteristic

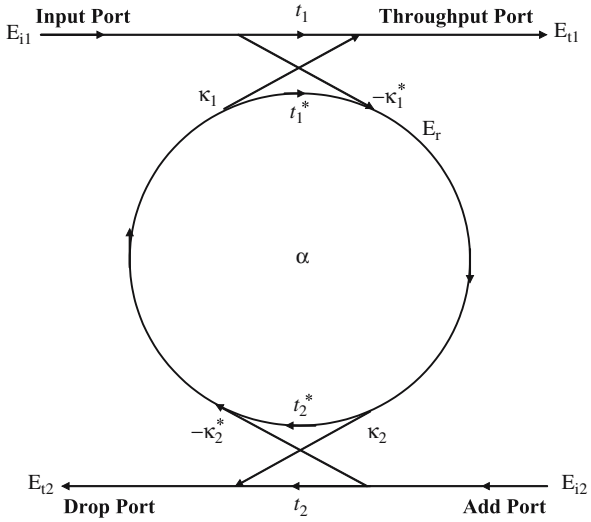

Fig. 2.4. Model of a basic add–drop single ring resonator filter

At resonance, the output power from the drop port is given by

$$P_{t2-\text{Resonance}} = |E_{t2-\text{Resonance}}|^2 = \frac{\left(1-|t_1|^2\right)\cdot\left(1-|t_2|^2\right)\cdot\alpha}{(1-\alpha\,|t_1 t_2|)^2} \tag{2.15}$$

The throughput port mode amplitude E_{t1} (2.13) will be zero at resonance for identical symmetrical couplers $t_1 = t_2$ if $\alpha = 1$, which indicates that the wavelength on resonance is fully extracted by the resonator. The value of $\alpha = 1$ can only be achieved by the implementation of gain incorporated in the ring resonator to compensate the waveguide losses. The value of the loss coefficient α is fixed in a purely passive ring resonator. A possibility of achieving minimum intensity ($P_{t1} = 0$) at resonance of the output transmission P_{t1} at the throughput port is to adjust the coupling parameters t_1, t_2 to the loss coefficient α. From (2.13) we obtain

$$\alpha = \left|\frac{t_1}{t_2}\right|. \tag{2.16}$$

If the ring resonator is lossless ($\alpha = 1$), then the couplers have to be symmetric in order to achieve minimum intensity. The transmission of a lossless ring resonator add drop filter with radius of $r = 148\,\mu\text{m}$ is shown in Fig. 2.5.

There are different kinds of requirements on the simulation of various kinds of ring resonator configurations. Starting of with the given equations satisfies most basic models. The ring model can for example be divided

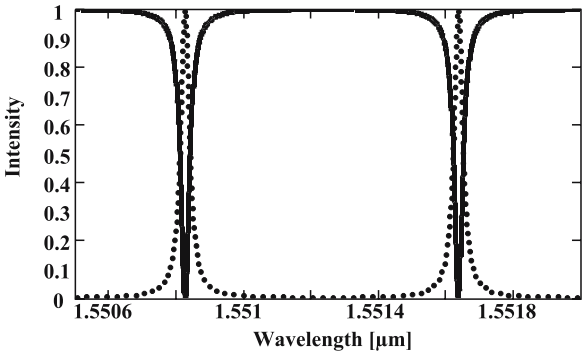

Fig. 2.5. Add–drop ring resonator filter characteristic

into more segments to account for different materials or modified waveguide paths. Examples of calculated models can be found in Rabus (2002) and Michelotti et al. (2004).

Ring Resonator Parameters

Ring resonator filters can be described by certain figures of merit which are also generally used to describe optical filters. One important figure is the distance between resonance peaks, which is called the free spectral range (FSR). A simple approximation can be obtained for the FSR by using the propagation constant from (2.4), neglecting the wavelength dependency of the effective refractive index

$$\frac{\partial\beta}{\partial\lambda} = -\frac{\beta}{\lambda} + k\frac{\partial n_{\mathrm{eff}}}{\partial\lambda} \approx -\frac{\beta}{\lambda}. \tag{2.17}$$

This leads to the FSR $\Delta\lambda$, which is the difference between the vacuum wavelengths corresponding to two resonant conditions.

$$\mathrm{FSR} = \Delta\lambda = -\frac{2\pi}{L}\left(\frac{\partial\beta}{\partial\lambda}\right)^{-1} \approx \frac{\lambda^2}{n_{\mathrm{eff}}L}. \tag{2.18}$$

Note that (2.18) is for the resonant condition next to a resonance found for the used propagation constant.

If the wavelength dependence of the effective index can not be neglected, it can be incorporated in the following way to obtain a modified version of (2.17).

$$\frac{\partial\beta}{\partial\lambda} = -\frac{k}{\lambda}n_{\mathrm{g}}, \tag{2.19}$$

where n_{g} is the group refractive index, which is defined as:

$$n_{\mathrm{g}} = n_{\mathrm{eff}} - \lambda\frac{\partial n_{\mathrm{eff}}}{\partial\lambda}. \tag{2.20}$$

The group refractive index can be used instead of the effective index whenever appropriate avoiding the approximation and obtaining more accurate values.

The modified FSR $\Delta\lambda$ is then given by

$$\mathrm{FSR} = \Delta\lambda = \frac{\lambda^2}{n_\mathrm{g} L}. \tag{2.21}$$

The next parameter of importance is the resonance width which is defined as the full width at half maximum (FWHM) or 3 dB bandwidth $2\delta\lambda$ of the resonance lineshape. Using the expressions for the drop port (2.14) and (2.15)

$$\left| \frac{-\kappa_1^* \kappa_2 \alpha_{1/2} \mathrm{e}^{\mathrm{j}\theta_{1/2}}}{1 - t_1^* t_2^* \alpha \mathrm{e}^{\mathrm{j}\theta}} \right|^2 = \frac{1}{2} \frac{|\kappa_1|^2 |\kappa_2|^2 \alpha}{(1 - \alpha |t_1 t_2|)^2}. \tag{2.22}$$

Assuming that the coupling coefficients are real, lossless, and without a phase term, (2.22) can be written as

$$\frac{\left(\kappa_1 \kappa_2 \alpha_{1/2}\right)^2}{1 - 2 t_1 t_2 \alpha \cos(\theta) + (t_1 t_2 \alpha)^2} = \frac{1}{2} \frac{\left(\kappa_1 \kappa_2 \alpha_{1/2}\right)^2}{(1 - t_1 t_2 \alpha)^2}. \tag{2.23}$$

Then

$$2 (1 - t_1 t_2 \alpha)^2 = 1 - 2 t_1 t_2 \alpha \cos(\theta) + (t_1 t_2 \alpha)^2. \tag{2.24}$$

For small θ, using the real part of the series expansion of the Euler formula

$$\cos(\theta) = 1 - \frac{\theta^2}{2}. \tag{2.25}$$

Therefore

$$\theta^2 = \frac{(1 - t_1 t_2 \alpha)^2}{t_1 t_2 \alpha}. \tag{2.26}$$

This equation can further be simplified if the loss in the ring is negligible and the coupling is symmetric ($t = t_1 = t_2$) to

$$\theta = \sqrt{\frac{(1 - t^2)^2}{t^2}} = \frac{1 - t^2}{t}. \tag{2.27}$$

Using (2.5) and (2.17) to translate into the wavelength domain

$$2\delta\lambda = \frac{\lambda^2}{\pi L n_\mathrm{eff}} \frac{1 - t^2}{t}. \tag{2.28}$$

The expression which is commonly used can be obtained by assuming weak coupling and $\lambda \gg \delta\lambda$

$$\mathrm{FWHM} = 2\delta\lambda = \frac{\kappa^2 \lambda^2}{\pi L n_\mathrm{eff}}. \tag{2.29}$$

Another parameter which can now be directly calculated from the parameters in the previous chapter is the finesse F of the ring resonator filter. It is defined as the ratio of the FSR and the width of a resonance for a specific wavelength (FWHM):

$$F = \frac{\mathrm{FSR}}{\mathrm{FWHM}} = \frac{\Delta\lambda}{2\delta\lambda} = \pi\frac{t}{1-t^2} \overset{\kappa\ll 1}{\approx} \frac{\pi}{\kappa^2}. \tag{2.30}$$

A parameter which is closely related to the finesse is the quality factor Q of a resonator, which is a measure of the sharpness of the resonance. It is defined as the ratio of the operation wavelength and the resonance width

$$Q = \frac{\lambda}{2\delta\lambda} = \pi\frac{n_{\mathrm{eff}}L}{\lambda}\frac{t}{1-t^2} = \frac{n_{\mathrm{eff}}L}{\lambda}F. \tag{2.31}$$

The quality factor can also be regarded as the stored energy divided by the power lost per optical cycle.

The intensity in the ring resonator can be much higher than that in the bus waveguides, as the traveling wave in the ring resonator interferes constructively at resonance with the input wave and thus the amplitude builds up. In addition to this intensity increase, the field also experiences a phase-shift of an integral multiple of 2π in one round trip. The intensity enhancement or buildup factor B is given by (for a configuration shown in Fig. 2.2)

$$B = \left|\frac{E_{i2}}{E_{i1}}\right|^2 = \left|\frac{-\alpha\kappa^*}{-\alpha t^* + \mathrm{e}^{-\mathrm{j}\theta}}\right|^2. \tag{2.32}$$

For a configuration like Fig. 2.4, the buildup factor is given by

$$B = \left|\frac{E_r}{E_{i1}}\right|^2 = \left|\frac{-\kappa_1^*}{1 - t_1^* t_2^* \alpha \mathrm{e}^{\mathrm{j}\theta}}\right|^2. \tag{2.33}$$

On resonance, the intensity enhancement factor is

$$B = \left|\frac{-\kappa_1^*}{1 - t_1^* t_2^* \alpha}\right|^2. \tag{2.34}$$

For a lossless resonator and setting $\kappa_1 = \kappa_2 = \kappa$ which is $\ll 1, B$ can be written as

$$B = \frac{1}{\kappa^2} \xrightarrow{(2.30)} \frac{F}{\pi}. \tag{2.35}$$

This equation directly relates the intensity enhancement factor B to the finesse F.

For the all-pass configuration and on resonance, the buildup factor is given by ($t_1 = t_2 = t$)

$$B = \frac{1+t}{1-t}. \tag{2.36}$$

Ring resonators can be used for nonlinear optical devices since the intensity in the resonator can be much higher than in the bus waveguide. Examples of devices utilizing nonlinearities in ring resonators are given in Sects. 5.7 and 5.8.

The Time-Dependent Relations

Before going on to extend the previous model incorporating additional ring resonators, the time-dependent relations are adapted from Little et al. (1997b) for the basic ring resonator add–drop configuration. Like in the previous model, it is assumed that the ring supports a traveling wave of amplitude $E(t)$, $P(t)$ represents the total power flowing through any cross section of the ring waveguide at time t. The ring is regarded as an oscillator of energy amplitude $e(t)$, normalized so that $p(t)$ represents the total energy stored in the ring. Energy and power in the ring are related through

$$p\left(t\right) = \left|e\left(t\right)\right|^2 = P\left(t\right)\frac{2\pi r}{v_\mathrm{g}}, \tag{2.37}$$

where v_g is the group velocity. The ring resonator has a resonant frequency of ω_R and amplitude decay time-constant of $1/\tau$. The decay rate and the power exciting the ring resonator are related to each other. The decay rate includes the power coupled to the transmitted wave $1/\tau_\mathrm{tr}$, the power lost due to intrinsic effects $1/\tau_\mathrm{ie}$, and power coupled to the output waveguide $1/\tau_{t2}$. This leads to

$$\frac{1}{\tau} = \frac{1}{\tau_\mathrm{tr}} + \frac{1}{\tau_\mathrm{ie}} + \frac{1}{\tau_{t2}}. \tag{2.38}$$

The time rate of change in ring energy can then be written as

$$\frac{\mathrm{d}}{\mathrm{d}t}e = \left(\mathrm{j}\omega_\mathrm{R} - \frac{1}{\tau}\right)e - \kappa^* \cdot E_{i1}. \tag{2.39}$$

The relation between the coupling parameter κ and the decay rates of the transmitted wave $1/\tau_\mathrm{tr}$ and the output waveguide $1/\tau_{t2}$, is determined by power conservation. The case is considered, when the ring resonator is excited to an energy of $|e_0|^2$, no output waveguide is present and no input wave E_{i1}. The ring energy, with no intrinsic loss, then decays as follow:

$$\left|e\left(t\right)\right|^2 = \left|e_0\right|^2 \exp\left(\frac{-2t}{\tau_\mathrm{tr}}\right). \tag{2.40}$$

From these set of eqs. (2.37–2.40), the power transfer characteristic for the drop port can be calculated with the input wave E_{i1} being proportional to $\exp(\mathrm{j}\omega t)$

$$e = \frac{-\mathrm{j}\sqrt{\dfrac{2}{\tau_\mathrm{tr}}}}{\mathrm{j}\left(\omega - \omega_\mathrm{R}\right) + \dfrac{1}{\tau}}E_{i1}. \tag{2.41}$$

From this equation, we can calculate the transmitted wave at the throughput port

$$E_{t1} = E_{i1} - \kappa^* e = \frac{\mathrm{j}\left(\omega - \omega_\mathrm{R}\right) + \frac{1}{\tau} + \mathrm{j}\kappa^* \sqrt{\frac{2}{\tau_\mathrm{tr}}}}{\mathrm{j}\left(\omega - \omega_\mathrm{R}\right) + \frac{1}{\tau}} E_{i1}. \tag{2.42}$$

Finally the drop port power transfer characteristic is obtained by using the equation for power conservation (note, $E_{i2} = 0$):

$$\left|E_{t2}\right|^2 = \left|E_{i1}\right|^2 - \left|E_{t1}\right|^2 = \frac{2}{\tau_{t2}} \left|e\right|^2 = \frac{\frac{4}{\tau_{t2}\tau_\mathrm{tr}}}{\left(\omega - \omega_\mathrm{R}\right)^2 + \frac{1}{\tau}} \left|E_{i1}\right|^2 \tag{2.43}$$

This equation can be simplified further if both waveguides couple equally to the ring, then $\tau_{t2} = \tau_\mathrm{tr}$.

The Z-Transform

Another approach to simulate ring resonator filters is by using the Z-transformation to describe the spectral and temporal response of ring resonator filters, described in detail in Madsen and Zhao (1999). Z-transform relationships for basic optical elements were first developed for fiber optic filters in Moslehi et al. (1984). This technique is used in pole-zero diagrams to design ring resonator filters in Kaalund and Peng (2004). In the following chapter, the Z-transform for the basic add–drop configuration (consisting of one ring resonator and two waveguides) is given which shall serve as a starting point for the calculation of more complex devices. Z-transforms are discussed extensively in the aforementioned literature on digital signal processing, therefore only a brief introduction is given here.

The Z-transform is an analytic extension of the discrete-time Fourier transform (DTFT) which converts a discrete time signal into a complex-variable frequency signal

$$H\left(z\right) = \sum_{n=-\infty}^{\infty} h\left(n\right) z^{-n}, \tag{2.44}$$

where z is a complex variable and $h(n)$ is the impulse response of a filter or the values of a discrete signal. Each term z^{-n} represents a delay. Of particular interest is when the absolute value of $|z| = 1$. This is called the unit circle in the complex plane where pole and zero locations of the function $H(z)$, which is evaluated along $z = exp(\mathrm{j}\omega)$, are plotted. In the case of ring resonator filters, $|z| = 1$ corresponds to resonant frequencies. A complete roundtrip of the unit circle corresponds to the FSR of the filter. Poles and zeros are related to the filter's frequency spectrum by their position on the complex plane. A zero positioned on the unit circle results in zero transmission at the frequency corresponding to the angle of this zero. A pole on the other hand on

the unit circle causes unity transmission at the corresponding frequency. As poles and zeros move away from the unit circle, their effect on the magnitude spectrum is reduced.

A linear discrete system with input signals x has the following output signal:

$$y(n) = b_0 x(n) + b_1 x(n-1) + \cdots + b_M x(n-M) - a_1 y(n-1), \\ - \cdots - a_N y(n-N). \tag{2.45}$$

The Z-transform for this type of filter is then given by

$$H(z) = \frac{\sum_{m=0}^{M} b_m z^{-m}}{1 + \sum_{n=1}^{N} a_n z^{-n}} = \frac{B(z)}{A(z)}. \tag{2.46}$$

$A(z)$ and $B(z)$ are Mth and Nth-order polynomials. The zeros z_m and poles p_n of $H(z)$ can be derived from the roots of the polynomials as follows:

$$H(z) = \frac{\Gamma z^{N-M} \sum_{m=1}^{M} (z - z_m)}{\sum_{n=1}^{N} (z - p_n)} = \frac{B(z)}{A(z)}, \tag{2.47}$$

where Γ is the gain of the filter. In passive filters, the transfer function can never be greater than 1, so Γ has a maximum value determined by $\max\{|\mathrm{H(z)}|_{\mathrm{z=exp(j\omega)}}\} = 1$ for these types of filters.

A ring resonator has a response which can be expressed in the form

$$H(z) = \sum_{n=0}^{\infty} a^n z^{-n} = \frac{1}{1 - az^{-1}}. \tag{2.48}$$

The basic configuration of an add–drop ring resonator filter (Fig. 2.4) is the simplest filter with a single pole response.

The sum of all optical paths for the drop port is given by

$$E_{t2}(z) = -\kappa_1 \kappa_2 \sqrt{\alpha z^{-1}} \left\{1 + t_1 t_2 \alpha z^{-1} + \cdots\right\} E_{i1}(z). \tag{2.49}$$

Using the Taylor series expansion, the equation can be simplified to give the drop port transfer function:

$$H_{21}(z) = \frac{E_{t2}(z)}{E_{i1}(z)} = \frac{-\kappa_1 \kappa_2 \sqrt{\alpha z^{-1}}}{1 - t_1 t_2 \alpha z^{-1}}. \tag{2.50}$$

There is a single pole at $t_1 t_2 \alpha$. As the matrix is symmetric, the transfer function $H_{21}(z)$ is equal to $H_{12}(z)$.

The sum of all optical paths for the throughput port resulting in its transfer function $H_{11}(z)$ is given by

$$\begin{aligned} E_{t1}(z) &= \left[t_1 - \kappa_1^2 t_2 \alpha z^{-1}\left\{1 + t_1 t_2 \alpha z^{-1} + \cdots\right\}\right] E_{i1}(z) \\ &= \left[t_1 - \frac{\kappa_1^2 t_2 \alpha z^{-1}}{1 - t_1 t_2 \alpha z^{-1}}\right] E_{i1}(z) \\ &= \left[\frac{t_1 - t_2 \alpha z^{-1}}{1 - t_1 t_2 \alpha z^{-1}}\right] E_{i1}(z), \\ \Rightarrow H_{11}(z) &= \frac{E_{t1}(z)}{E_{i1}(z)} = \frac{t_1 - t_2 \alpha z^{-1}}{1 - t_1 t_2 \alpha z^{-1}}. \end{aligned} \tag{2.51}$$

Similarly, the transfer function $H_{22}(z)$ can be derived to be

$$H_{22}(z) = \frac{E_{t2}(z)}{E_{i2}(z)} = \frac{t_2 - t_1 \alpha z^{-1}}{1 - t_1 t_2 \alpha z^{-1}}. \tag{2.52}$$

The obtained results for each transfer function can be expressed in two different matrix forms. The first form relates the input ports to the output ports and is called the scattering matrix (see also (2.1)) which is given by

$$\begin{pmatrix} E_{t1}(z) \\ E_{t2}(z) \end{pmatrix} = S_{\mathrm{RR}}(z) \begin{pmatrix} E_{i1}(z) \\ E_{i2}(z) \end{pmatrix}, \tag{2.53}$$

$$S_{\mathrm{RR}}(z) = \begin{pmatrix} \dfrac{t_1 - t_2 \alpha z^{-1}}{1 - t_1 t_2 \alpha z^{-1}} & \dfrac{-\kappa_1 \kappa_2 \sqrt{\alpha z^{-1}}}{1 - t_1 t_2 \alpha z^{-1}}, \\ \dfrac{-\kappa_1 \kappa_2 \sqrt{\alpha z^{-1}}}{1 - t_1 t_2 \alpha z^{-1}} & \dfrac{t_2 - t_1 \alpha z^{-1}}{1 - t_1 t_2 \alpha z^{-1}} \end{pmatrix}.$$

The second form relates the quantities in one plane to the ones in another plane as can be seen in Fig. 2.6. This type of matrix is called the transfer matrix which is given by

$$\begin{pmatrix} E_{i1}(z) \\ E_{t1}(z) \end{pmatrix} = \Phi_{\mathrm{RR}}(z) \begin{pmatrix} E_{i2}(z) \\ E_{t2}(z) \end{pmatrix}, \tag{2.54}$$

$$\Phi_{\mathrm{RR}}(z) = \frac{1}{-\kappa_1 \kappa_2 \sqrt{\alpha z^{-1}}} \begin{pmatrix} 1 - t_1 t_2 \alpha z^{-1} & -t_2 + t_1 \alpha z^{-1} \\ t_1 - t_2 \alpha z^{-1} & 1 + \kappa_1 \kappa_2 \alpha z^{-1} \end{pmatrix}.$$

The scattering matrix form is used to express the implication of power conservation and reciprocity. The transfer matrix form is used for describing multistage filters. It is therefore also referred to as the chain matrix. This type of transfer matrix is suitable to describe multiple serially coupled ring resonators. The transfer matrix to be used for describing multiple parallel coupled resonators has the form (Grover et al. 2002)

$$\begin{pmatrix} E_{i1}(z) \\ E_{t2}(z) \end{pmatrix} = \Phi'_{\mathrm{RR}}(z) \begin{pmatrix} E_{t1}(z) \\ E_{i2}(z) \end{pmatrix}, \tag{2.55}$$

$$\Phi'_{\mathrm{RR}}(z) = \frac{1}{t_1 - t_2 \alpha z^{-1}} \begin{pmatrix} 1 - t_1 t_2 \alpha z^{-1} & \kappa_1 \kappa_2 \sqrt{\alpha z^{-1}} \\ -\kappa_1 \kappa_2 \sqrt{\alpha z^{-1}} & t_1 t_2 - \alpha z^{-1} \end{pmatrix}.$$

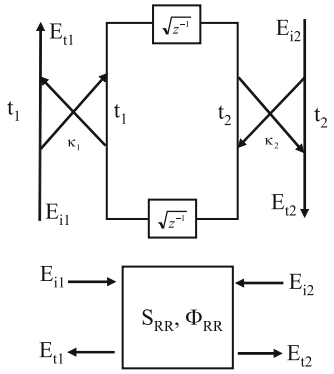

Fig. 2.6. Z-transform layout of an add–drop ring resonator filter

Using the different simulation techniques described in this chapter it is possible to build a simulation model for all relevant lateral and vertically coupled ring resonator filter configurations.

Incorporating Loss in Ring Resonator Filters

In the previous simulation models, loss is basically included by insertion of the parameter α in the formulas. Loss in ring resonator filters scales the spectral curves without changing them significantly if the loss is not too large. Different types of losses have been considered and described in literature to account for various fabrication methods and tolerances. A few examples will be given in the following paragraph to give a starting point for the calculation and simulation of losses in ring resonators.

A loss which is most obvious is the radiation loss which occurs in the curved section of ring resonators (Chin and Ho 1998). The radiation loss will become large for a large surface roughness. The surface roughness on the other hand can induce contradirectional coupling which can degrade the performance of a ring resonator filter and can even cause a splitting of the resonant peak (Little et al. 1997a). The calculation of the radiation and scattering losses in ring resonators is presented in detail in Rabiei (2005). Here a perturbative method for the calculation of losses due to an arbitrary variation in the refractive index of the core or due to an arbitrary variation in the shape of ring resonator is described.

Loss in ring resonator devices can also be used advantageously as was demonstrated using (2.16). An analysis of how loss and gain can be used to tune, trim, or compensate the wavelength response of ring resonator filters is described in Little and Chu (2000).

In the following chapter the basic model of a ring resonator is extended to analyze a racetrack shaped ring resonator.

2.1.2 Racetrack-Shaped Resonators

The equations in the previous chapter described the general behavior of a basic ring resonator filter. However to simulate certain ring resonator configurations, this set of equations has to be extended. In a waveguide-coupled ring resonator filter, the coupling gap size is determined by the amount of coupling required and the coupling length available. Using lateral coupling, a larger gap is desirable as it increases the fabrication tolerance. In this case, for a given coupling coefficient, the gap size can be enlarged if the coupling distance is increased to obtain a racetrack-shaped ring resonator (Fig. 2.7).

The coupling distance can be increased by using a lateral or vertical geometry (Chin and Ho 1998). In the case of the racetrack shaped ring resonator, the coupling distance is approximately the length of the straight sections (if no coupling occurs before the actual coupler region starts), which are tangential to the circular arcs at output and input ports. At the transitions between the curved and the straight sections, the mode will change adiabatically between the radial mode in a curved waveguide and the normal mode in a straight waveguide. As the straight sections are lengthened the radius of the curved sections must be reduced if the total cavity length is to remain constant. This cannot always be achieved in practical applications.

In the case of racetrack resonators, it is important to consider the variation of phase difference φ which occurs in the coupling region in both couplers between t and κ. The phase difference is length-dependent and affects the output characteristics, not only in the magnitude but also in the resonant conditions. This phase difference can be implemented in (2.13) and (2.14) using the method described in Lee et al. (2004).

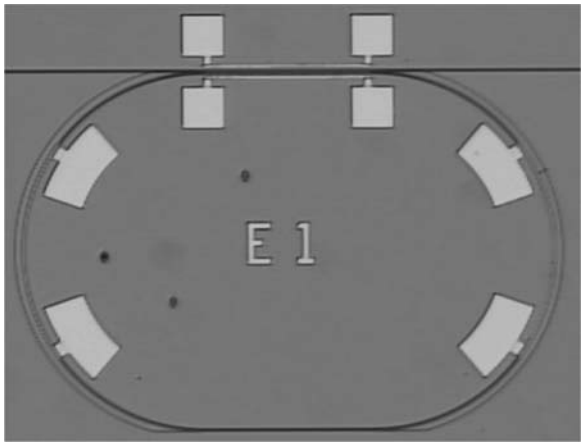

Fig. 2.7. A racetrack-shaped ring resonator filter with integrated platinum resistors on top of the curved sections and the coupler (contact pads visible)

For the throughput port:

$$E_{t1} = \frac{t_1 \mathrm{e}^{\mathrm{j}\varphi_{t1}} - t_2^* \alpha_{1/2}^2 \mathrm{e}^{\mathrm{j}\theta} \left(t_1 t_1^* \mathrm{e}^{\mathrm{j}2\varphi_{t1}} - \kappa_1 \kappa_1^* \mathrm{e}^{-\mathrm{j}2\varphi_{\kappa 2}} \right) \mathrm{e}^{\mathrm{j}\varphi_{t2}}}{1 - t_1^* t_2^* \alpha_{1/2}^2 \mathrm{e}^{\mathrm{j}\theta} \mathrm{e}^{\mathrm{j}\varphi_{t1}} \mathrm{e}^{\mathrm{j}\varphi_{t2}}}. \tag{2.56}$$

For the drop port

$$E_{t2} = \frac{-\kappa_1^* \kappa_2 \alpha_{1/2} \mathrm{e}^{\mathrm{j}\theta_{1/2}} \mathrm{e}^{-\mathrm{j}\varphi_{\kappa 1}} \mathrm{e}^{-\mathrm{j}\varphi_{\kappa 2}}}{1 - t_1^* t_2^* \alpha \mathrm{e}^{\mathrm{j}\theta} \mathrm{e}^{\mathrm{j}\varphi_{t1}} \mathrm{e}^{\mathrm{j}\varphi_{t2}}}. \tag{2.57}$$

The resonant condition $(\theta + \varphi_{t1} + \varphi_{t2}) = 2\pi m$ has changed slightly compared to (2.9). The output transmission at resonance is no longer independent of t and κ which can be seen comparing the relevant terms in (2.50) and (2.51). This leads to a significant performance change and confirms the importance of taking into account the phase difference when analyzing racetrack shaped ring resonator configurations. The phase difference is not only of importance in directional couplers, but also in MMI couplers. An analysis of a racetrack shaped ring resonator add–drop filter having two MMI couplers is given in Caruso and Montrosset (2003). The MMI length should be selected in order to satisfy the $\pi/2$ relation between the phases of the transmission and the coupling terms to obtain a symmetric transmission characteristic of the throughput and of the drop port. If the $\pi/2$ relation is not satisfied, a strong asymmetry in the transmission characteristic will be obtained.

A further description of the implementation of directional and MMI couplers in ring resonators is given in Sect. 4.1.

2.2 Double Ring Resonators

Double ring resonators offer the possibility of realizing a "box-like" filter characteristic which is favorably used in optical networks. This is not the only advantage, but also from the point of characterization, two rings if coupled in series have the drop port in the same direction as the input port, which is also convenient for interconnection of many 2×2 devices. Serially and parallel coupled ring resonator configurations have been described in detail in Chu et al. (1999a); Little et al. (1997b, 2000a); Melloni (2001) and Emelett and Soref (2005).

In the serially coupled configuration, each ring resonator is coupled to one another, and a signal that is to be dropped from the input port to the drop port must pass sequentially through each resonator. Because of this sequential power transfer, all resonators must be precisely resonant at a common wavelength. The resulting resonant line shape in the series configuration is determined physically by the separations between the ring resonators. In the parallel-coupled configuration, all resonators are coupled to both the input and drop port waveguides, but usually not directly to one another (the resonators can also be coupled to one another resulting in a wavelength selective

reflector as is described in Sects. 2.2.2 and 2.3.1). The resonators are instead indirectly coupled to each other by the optical path lengths along the input and output waveguides that interconnect them. These lengths determine the details of the resonant line shapes. An optical signal in the parallel configuration passes through all ring resonators simultaneously. This softens the requirement that the resonances of each ring have to be precisely identical. Nonaligned resonant frequencies instead lead to multiple peaks, or ripple in the lineshape.

The ready to use transfer functions of serially and parallel coupled double ring resonators will be described in the following sections.

2.2.1 Serially Coupled Double Ring Resonator

The schematic of a serially coupled double ring resonator is depicted in Fig. 2.8.

From this model and using the same procedure as in Sect. 2.1.1 the fields depicted in Fig. 2.8 can be calculated as follows:

$$E_{1a} = -\kappa_1^* E_{i1} + t_1^* \alpha_1 \mathrm{e}^{\mathrm{j}\frac{\theta_1}{2}} E_{1b}, \tag{2.58}$$

$$E_{1b} = t_2^* \alpha_1 \mathrm{e}^{\mathrm{j}\frac{\theta_1}{2}} E_{1a} - \kappa_2^* \alpha_2 \mathrm{e}^{\mathrm{j}\frac{\theta_1}{2}} E_{2b}, \tag{2.59}$$

$$E_{2a} = \kappa_2 \alpha_1 \mathrm{e}^{\mathrm{j}\frac{\theta_2}{2}} E_{1a} + t_2 \alpha_2 \mathrm{e}^{\mathrm{j}\frac{\theta_2}{2}} E_{2b}, \tag{2.60}$$

$$E_{2b} = -\kappa_3^* E_{i2} + t_3^* \alpha_2 \mathrm{e}^{\mathrm{j}\frac{\theta_2}{2}} E_{2a} \tag{2.61}$$

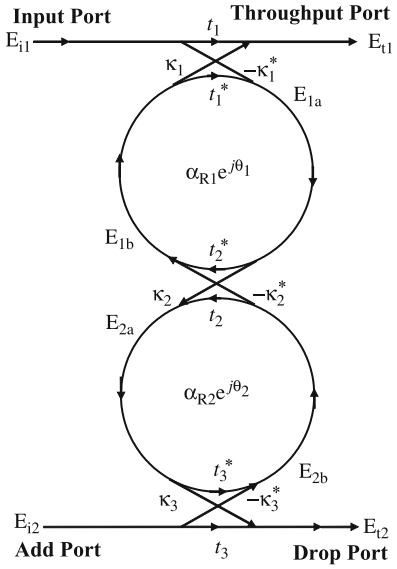

Fig. 2.8. Two ring resonators coupled in series

$$E_{t1} = t_1 E_{i1} + \kappa_1 \alpha_1 \mathrm{e}^{\mathrm{j}\frac{\theta_1}{2}} E_{1b}, \tag{2.62}$$

$$E_{t2} = t_3 E_{i2} + \kappa_3 \alpha_2 \mathrm{e}^{\mathrm{j}\frac{\theta_2}{2}} E_{2a}, \tag{2.63}$$

where $\alpha_{1,2} = \alpha_{\mathrm{R1}_{1/2},R2_{1/2}}$ represent the half round trip loss coefficients of ring resonator one and two respectively. From (2.58) to (2.63) the general expressions for the transfer functions for the throughput and the drop port can be derived. A simplified form can be obtained by assuming a coupler without losses and symmetric coupling behavior, setting $t = t^*$ and $\kappa = -\kappa^*$ (note that the phase factor $-\mathrm{j}$ has not been introduced into the assumption and can be added if required) which gives the ready to use amplitude forms for the throughput port ($E_{i2} = 0$)

$$\frac{E_{t1}}{E_{i1}} = \frac{-t_1 \kappa_1^2 \alpha_1 \mathrm{e}^{\mathrm{j}\theta_1} \left(t_3 \alpha_2 \mathrm{e}^{\mathrm{j}\theta_2} - t_2\right)}{1 - t_3 t_2 \alpha_2 \mathrm{e}^{\mathrm{j}\theta_2} - t_2 t_1 \alpha_1 \mathrm{e}^{\mathrm{j}\theta_1} + t_3 t_1 \alpha_1 \alpha_2 \mathrm{e}^{\mathrm{j}\theta_1} \mathrm{e}^{\mathrm{j}\theta_2}} \tag{2.64}$$

and for the drop port:

$$\frac{E_{t2}}{E_{i1}} = \frac{\kappa_3 \kappa_2 \kappa_1 \alpha_1 \alpha_2 \mathrm{e}^{\mathrm{j}\frac{\theta_1}{2}} \mathrm{e}^{\mathrm{j}\frac{\theta_2}{2}}}{1 - t_3 t_2 \alpha_2 \mathrm{e}^{\mathrm{j}\theta_2} - t_2 t_1 \alpha_1 \mathrm{e}^{\mathrm{j}\theta_1} + t_3 t_1 \alpha_1 \alpha_2 \mathrm{e}^{\mathrm{j}\theta_1} \mathrm{e}^{\mathrm{j}\theta_2}}. \tag{2.65}$$

For realizing a double ring resonator with maximally flat response, first the input/output waveguide ring coupling coefficient $\kappa_1(\kappa_3)$ has to be determined. To simplify the model further, it is defined that the input/output waveguide-ring coupling coefficients $\kappa_1 = \kappa_3$. The calculation of the coupling coefficients to obtain the appropriate coupling values between the two ring resonators in order to achieve maximally flat response can be made according to Emelett and Soref (2005), Little et al. (1997b) by using the geometry and index profile shown in Fig. 2.9, where two coupled waveguides of width $2w_p$ and $2w_q$ with indexes of n_p and n_q, surrounded by a cladding of n_0, at the plane of smallest separation $2s_0$, defined as the center to center gap are shown.

The approximate coupling coefficient is then given by

$$\kappa = \frac{\omega \varepsilon_0 \cos\left(k_{x_{p,q}} w_q\right)}{2\sqrt{P_p P_q}\left(k_{x_p}^2 + \alpha_q^2\right)} \left(n_p^2 - n_0^2\right) \sqrt{\frac{\pi R}{\alpha_q}} \mathrm{e}^{[\alpha_q (w_q - 2s_0)]} \times \left\{\alpha_q \cos\left(k_{x_p} w_p\right) \sinh\left(\alpha_q w_p\right) + k_{x_p} \sin\left(k_{x_p} w_p\right) \cosh\left(\alpha_q w_p\right)\right\}. \tag{2.66}$$

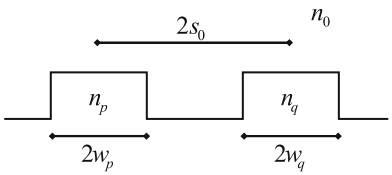

Fig. 2.9. Index profile and geometry of coupled waveguides

Using

$$P_{p,q} = \frac{\beta_{p,q}}{2\omega\mu_0}\left(w_{p,q} + \frac{1}{\alpha_{p,q}}\right), \tag{2.67}$$

$$k_{x_{p,q}} = \sqrt{n_{p,q}^2 k^2 - \beta_{p,q}^2}, \tag{2.68}$$

$$\alpha_{p,q} = \sqrt{\beta_{p,q}^2 - n_0^2 k^2}, \tag{2.69}$$

where $P_{p,q}$ is the mode power, $k_{x_{p,q}}$ is the transverse propagation constant of the core, and $\alpha_{p,q}$ is the decay constant in the cladding, $\beta_{p,q}$ is the propagation constant, ω is the circular frequency, ε_0 is the permittivity of free space, all within waveguide p or q. The refractive index n_0 of the surrounding media is set equal to 1 (air). The coefficient R is defined as the effective radius of curvature of the ring and is given by:

$$R = \frac{r_1 r_2}{r_1 + r_2}, \tag{2.70}$$

where $r_{1,2}$ represents the radius of ring one and two respectively. The radii of the rings are chosen to satisfy the 2π phase shift condition with the completion of one round trip in the ring resonator which is given by:

$$m\lambda_m = 2\pi r_{1,2} n_{\text{eff}}. \tag{2.71}$$

In order to realize a flat passband, the analysis of the power loss ratio, which is the ratio of total input power to power present at the detected port, is required. The power loss ratio in polynomial form is given by

$$P_{LR} = \left|\frac{E_i}{E_{t2}}\right|^2 = 1 + \frac{1}{\mu_1^4 \mu_2^4}\left[\Delta\omega^4 + \left(\frac{\mu_1^4}{2} - 2\mu_2^2\right)\Delta\omega^2 + \left(\mu_2^2 - \frac{\mu_1^4}{4}\right)^2\right], \tag{2.72}$$

where $\Delta\omega$ is the frequency deviation which is related to the resonant frequency ω_m by

$$\Delta\omega = \omega - \omega_m. \tag{2.73}$$

The coefficient μ is the fractional power coupled. It is given by

$$\mu_1^2 = \frac{\kappa_1^2 v_{g1}}{2\pi r_1} \text{ and } \mu_2^2 = \frac{\kappa_2^2 v_{g1} v_{g2}}{4\pi^2 r_1 r_2}. \tag{2.74}$$

The goal of realizing a maximally flat response is obtained when the power loss ratio is zero at the defined resonance. This is the case for

$$\mu_2^2 = 0.250\mu_1^4. \tag{2.75}$$

Assuming identical rings, this leads to the coupling coefficient

$$\kappa_2^2 = 0.250\kappa_1^4. \tag{2.76}$$

Using these equations, it is possible to design a double ring resonator filter with maximally flat response for the drop port.

A serially coupled double ring resonator opens up the possibility of expanding the FSR to the least common multiple of the FSR of individual ring resonators. This is done by choosing different radii in the double ring resonator. In the case of different radii, the light passing through the double ring resonator is launched from the drop port when the resonant conditions of both single ring resonators are satisfied. The FSR of the double ring resonator with two different radii is expressed by

$$\mathrm{FSR} = \mathrm{N} \cdot \mathrm{FSR}_1 = \mathrm{M} \cdot \mathrm{FSR}_2, \tag{2.77}$$

which leads to

$$\mathrm{FSR} = |\mathrm{M} - \mathrm{N}| \, \frac{\mathrm{FSR}_1 \cdot \mathrm{FSR}_2}{|\mathrm{FSR}_1 - \mathrm{FSR}_2|}, \tag{2.78}$$

where N and M are natural and coprime numbers.

The use of two ring resonators with different radii opens the possibility to realize a larger FSR than would be achieved using only a single ring resonator. The transmission characteristic of the throughput port has mainly a Lorentzian shape. A box-like filter response using two different radii can only be realized by using two parallel coupled double ring resonators ($R_1 \neq R_2$). The use of such configurations as optical filters is limited by unwanted additional resonant peaks. Investigations on these types of filters have been performed in Suzuki et al. (1995), Sorel et al. (1999). Different types of waveguide coupled ring resonator configurations to expand the free spectral range have been analyzed in Hidayat et al. (2003).

2.2.2 Parallel Coupled Double Ring Resonator

The schematic of a parallel coupled double ring resonator is shown in Fig. 2.10.

From this model, the fields in Fig. 2.10 can be calculated as follows:

$$E_{1a} = -\kappa_1^* E_{i1} + t_1^* \alpha_1 \mathrm{e}^{\mathrm{j}\frac{\theta_1}{2}} E_{1b}, \tag{2.79}$$

$$E_{1b} = t_2^* \alpha_1 \mathrm{e}^{\mathrm{j}\frac{\theta_1}{2}} E_{1a} - \kappa_2^* \mathrm{e}^{\mathrm{j}\theta_W} \left(\kappa_4 \alpha_2 \mathrm{e}^{\mathrm{j}\frac{\theta_2}{2}} E_{2a} - t_4 E_{i2} \right), \tag{2.80}$$

$$E_{2a} = -\kappa_3^* \mathrm{e}^{\mathrm{j}\theta_W} \left(t_1 E_{i1} + \kappa_1 \alpha_1 \mathrm{e}^{\mathrm{j}\frac{\theta_1}{2}} E_{1b} \right) + t_3^* \alpha_2 \mathrm{e}^{\mathrm{j}\frac{\theta_2}{2}} E_{2b}, \tag{2.81}$$

$$E_{2b} = -\kappa_4^* E_{i2} + t_4^* \alpha_2 \mathrm{e}^{\mathrm{j}\frac{\theta_2}{2}} E_{2a}, \tag{2.82}$$

$$E_{t1} = t_3 \mathrm{e}^{\mathrm{j}\theta_W} \left(t_1 E_{i1} + \kappa_1 \alpha_1 \mathrm{e}^{\mathrm{j}\frac{\theta_1}{2}} E_{1b} \right) + \kappa_3 \alpha_2 \mathrm{e}^{\mathrm{j}\frac{\theta_2}{2}} E_{2b}, \tag{2.83}$$

$$E_{t2} = t_2 \mathrm{e}^{\mathrm{j}\theta_W} \left(t_4 E_{i2} + \kappa_4 \alpha_2 \mathrm{e}^{\mathrm{j}\frac{\theta_2}{2}} E_{2a} \right) + \kappa_2 \alpha_1 \mathrm{e}^{\mathrm{j}\frac{\theta_1}{2}} E_{1a} \tag{2.84}$$

$$\theta_W = k_W \cdot n_{\mathrm{Weff}} \cdot \Lambda, \tag{2.85}$$

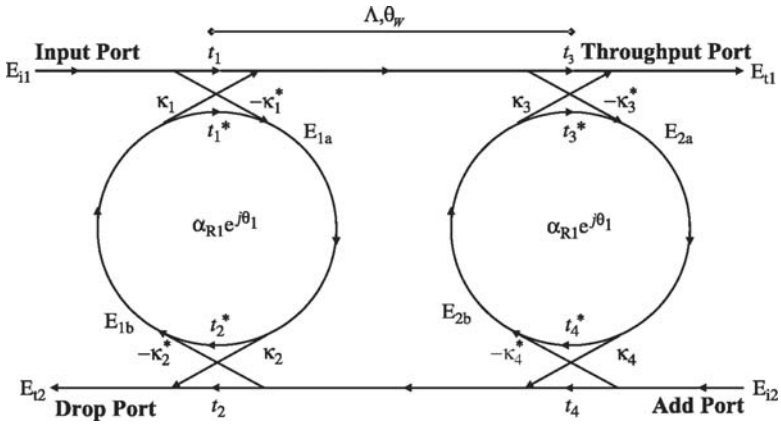

Fig. 2.10. Parallel coupled double ring resonator

where θ_{W} is the phase shift introduced by the segment of length Λ with effective refractive index n_{Weff} of the input waveguide joining both ring resonators.

From (2.79) to (2.85) the general expressions for the transfer functions for the throughput and the drop port can be derived. A simplified form can again be obtained by assuming couplers and bus waveguides without losses and symmetric coupling behavior, setting $t = t^*$ and $\kappa = -\kappa^*$ (note that the phase factor $-\mathrm{j}$ has not been introduced into the assumption and can be added if required) which gives the amplitude forms for the throughput port ($E_{i2} = 0$)

$$\frac{E_{t1}}{E_{i1}} = t_3 t_1 \mathrm{e}^{\mathrm{j}\theta_W} + t_3 \kappa_1 \alpha_1 \mathrm{e}^{\mathrm{j}\theta_W \frac{\theta_1}{2}} \left[h + \frac{f\,(a+bc)}{1-d} \right] + \kappa_3 t_4 \alpha_2^2 \mathrm{e}^{\mathrm{j}\theta_2} \frac{a+bc}{1-d}. \quad (2.86)$$

And for the drop port

$$\frac{E_{t2}}{E_{i1}} = \kappa_1 \kappa_2 \alpha_1 \mathrm{e}^{\mathrm{j}\frac{\theta_1}{2}} + \kappa_2 t_1 \alpha_1^2 \mathrm{e}^{\mathrm{j}\theta_1} \left[h + \frac{f\,(a+bc)}{1-d} \right] + t_2 \kappa_4 \alpha_2 \mathrm{e}^{\mathrm{j}\theta_W \frac{\theta_2}{2}} \frac{a+bc}{1-d}, \quad (2.87)$$

where

$$a = \frac{\kappa_3 t_1 \mathrm{e}^{\mathrm{j}\theta_W}}{1 - t_3 t_4 \alpha_2^2 \mathrm{e}^{\mathrm{j}\theta_2}}, \quad (2.88)$$

$$b = \frac{\kappa_1 \alpha_1 \mathrm{e}^{\mathrm{j}\frac{\theta_1}{2}}}{1 - t_3 t_4 \alpha_2^2 \mathrm{e}^{\mathrm{j}\theta_2}}, \quad (2.89)$$

$$c = \frac{\kappa_1 t_2 \alpha_1 \mathrm{e}^{\mathrm{j}\frac{\theta_1}{2}}}{1 - t_1 t_2 \alpha_1^2 \mathrm{e}^{\mathrm{j}\theta_1}} \quad (2.90)$$

$$f = \frac{\kappa_2 \kappa_4 \alpha_2 \mathrm{e}^{\mathrm{j}\theta_W \frac{\theta_2}{2}}}{1 - t_1 t_2 \alpha_1^2 \mathrm{e}^{\mathrm{j}\theta_1}}, \tag{2.91}$$

$$h = \frac{\kappa_1 t_2 \alpha_1 \mathrm{e}^{\mathrm{j}\frac{\theta_1}{2}}}{1 - t_1 t_2 \alpha_1^2 \mathrm{e}^{\mathrm{j}\theta_1}}. \tag{2.92}$$

$$d = b \cdot f \tag{2.93}$$

Similar to the serially coupled double ring resonator, it is possible to increase the overall FSR of this configuration by adjusting the length of the waveguide joining the two ring resonators.

The parallel configuration can be treated as a grating. Constructive interference of the reflected waves from each ring resonator is obtained by choosing Λ to be equal to an odd multiple of a quarter wavelength.

$$\Lambda = (2m + 1)\, \frac{\lambda_0}{4 n_{\mathrm{Weff}}}, \tag{2.94}$$

where λ_0 is the center wavelength of the passband.

If the length Λ is chosen such that the FSR of the ring resonators and the FSR of the "grating" obey the following condition:

$$\mathrm{FSR} = \mathrm{N_{Ring}} \cdot \mathrm{FSR_{Ring}} = \mathrm{M_{Grating}} \cdot \mathrm{FSR_{Grating}}. \tag{2.95}$$

The Vernier effect (Griffel 2000b) causes the transmission peaks of the ring resonators within the overall obtained FSR to be suppressed, which results in a larger FSR than would be achieved for a single ring resonator. The distance between the resonators can be calculated in this case using:

$$\Lambda = \frac{M_{grating} n_{\mathrm{eff}}}{N_{\mathrm{Ring}} n_{\mathrm{Weff}}} \pi r. \tag{2.96}$$

These set of equations can of course be transferred to multiple coupled parallel ring resonator configurations as will be shown in Sect. 2.3.

Parallel Coupled Double Ring Resonator with Coupling Between the Two Ring Resonators

A special double ring resonator configuration is obtained, when coupling between the two ring resonators is allowed (Fig. 2.11). The reflective properties of such a device have been analyzed in Chremmos and Uzunoglu (2005) and the following transfer functions are based on this reference. A similar wavelength reflective filter consisting of four interacting ring resonators has been presented in Poon, Scheuer, Yariv (2004e) which is going to be described in Sect. 2.3.1.

Using the fields and coupling coefficient in Fig. 2.11, it is possible to derive the general expressions for describing the transfer characteristics of this type of configuration.

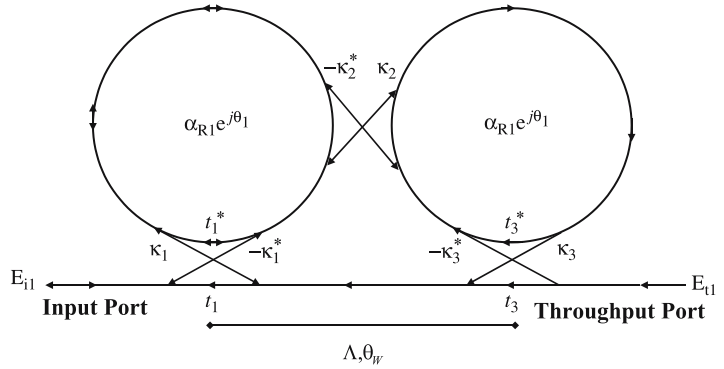

Fig. 2.11. Double ring resonator with inter ring coupling

A simplified expression for the reflectivity at port E_{i1} (denoted by the symbol $\leftarrow$ as the superscript) is obtained for the lossless case and symmetric coupling coefficients between the ring resonator and the bus waveguide ($\kappa = \kappa_1 = \kappa_3$):

$$\left|\overleftarrow{E}_{i1}\right|^2 = \frac{4\left(\frac{\kappa_2\kappa^2}{2t}\right)^2\left(\cos\theta - \frac{t_2\left(1+t^2\right)}{2t}\right)^2}{\left[\left(\cos\theta - \frac{t_2\left(1+t^2\right)}{2t}\right)^2 + \left(\frac{\kappa_2\kappa^2}{2t}\right)^2\right]^2}. \tag{2.97}$$

The phase factor for the distance Λ between the rings does not appear and therefore does not have an influence on the transfer characteristic. This is a special property of the double coupled configuration and does not apply for multiple serially coupled ring resonators. Different reflectivity profiles can be realized using appropriate coupling coefficients. Weakly coupled ring resonators lead to single reflection peaks in the reflectivity function where the height of the peak depend on the value of the coupling coefficients. In order to realize a maximally flat response with a single peak, the coupling coefficients have to obey the following equation:

$$\kappa_2 = \frac{\kappa^2}{\sqrt{2}\left(1+t^2+\sqrt{2}t\right)}. \tag{2.98}$$

The corresponding FWHM is given by

$$\mathrm{FWHM} = 4\sin^{-1}\left(\kappa\sqrt{\frac{\kappa_2}{2^{\frac{3}{2}}t}}\right). \tag{2.99}$$

The expression for the reflectivity at port E_{i1} incorporating loss parameter α is given by

$$\left|\overleftarrow{E}_{i1}\right|^2 = \frac{\left(\dfrac{\kappa_2\kappa^2\left(\alpha^2+1\right)}{2\alpha t}\right)^2}{\left[\left(\cos\theta - \dfrac{t_2\left(1+\alpha^2t^2\right)}{2\alpha t}\right)^2 + \left(\dfrac{\kappa_2\left(1-\alpha^2t^2\right)^2}{2\alpha t}\right)^2\right]^2} \times \left[\begin{array}{l}\left(\cos\theta - \dfrac{t_2\left(1+\alpha^2t^2\right)}{2\alpha t} + \dfrac{t_2}{2\alpha t}\dfrac{\left(1-\alpha^2\right)\left(1-\alpha^2t^2\right)}{1+\alpha^2}\right)^2 \\ + \left(\dfrac{1-\alpha^2}{1+\alpha^2}\right)\sin^2\theta\end{array}\right]. \tag{2.100}$$

So far ready to use transfer functions for single and double ring resonator configuration have been presented. In the following chapter, different calculation methods are presented to derive the transfer function of different types of multiple coupled ring resonators.

2.3 Multiple Coupled Resonators

The use of multiple vertical or lateral coupled ring resonator configurations opens up the possibility to realize custom designed transmission functions and thus is suitable for a wide variety of device implementations (Schwelb and Frigyes 2001). Vertical and lateral ring resonator architectures where the rings are either coupled in series or in parallel have been implemented in the past. A detailed theoretical analysis of a vertically stacked multiple coupled ring resonator, where the ring resonators are on top of each other is presented in Sumetsky (2005). The use of multiple coupled ring resonator configurations together with other photonic devices like grating couplers or Mach–Zehnder interferometers increases the functionality and transmission characteristic even further (Weiershausen and Zengerle 1996). One of the main targets of realizing optical filters is to tailor the passband shape. In analogy to electronic filter design, Butterworth (1930) and Chebyshev type of optical filters are preferred. Butterworth filters are maximally flat and do not have any ripples in the passband. The shape of the transfer function does not change for higher order filters except that the roll off becomes steeper as the order of the filter increases. Chebyshev filters have a steeper roll off than Butterworth type of filters and have ripples either in the passband or stopband which distinguishes Chebyshev type I and type II filters. The square magnitude response of a Butterworth filter has the form (Madsen and Zhao 1999)

$$\left|H_N\left(x\right)\right|^2 = \frac{1}{1+\left(\dfrac{x}{x_0}\right)^{2N}}, \tag{2.101}$$

where x_0 is the 3 dB cutoff frequency.

The response of Chebyshev type I and II filters have the form (Madsen and Zhao 1999)

$$\text{Type I}$$

$$|H_N(x)|^2 = \frac{1}{1 + y^2 T_N^2\left(\dfrac{x}{x_C}\right)} \tag{2.102}$$

$$T_N(x) = \begin{cases} \cos\left(N \cos^{-1} x\right) & \text{for} \quad |x| \le 1 \\ \cosh\left(N \cosh^{-1} x\right) & \text{for} \quad |x| > 1 \end{cases},$$

$$\text{Type II}$$

$$|H_N(x)|^2 = \frac{1}{1 + y^2 \left[\dfrac{T_N^2\left(\dfrac{x_S}{x_P}\right)}{T_N^2\left(\dfrac{x_S}{x}\right)}\right]}, \tag{2.103}$$

where $T_N(x)$ is the Nth-order Chebyshev polynomial, y determines the passband ripples, x_C is the center frequency of the filter, x_P and x_S define the changeover region on the passband and stopband, respectively.

2.3.1 Serially Coupled Ring Resonators

One of the first papers to present a calculation method for serially coupled ring resonator synthesis is Orta et al. (1995). The method is based on the Z-transformation using the transfer matrix (see (2.54)). The Z-transformation has also been used in Madsen and Zhao (1996) to simulate and fabricate a serially coupled ring resonator filter. The transfer matrix method has also been used in Melloni and Martinelli (2002) and Poon et al. (2004c) for simulating and designing various serially coupled ring resonator configurations. Serially coupled ring resonators are also referred to as coupled-resonator optical waveguides (CROW) Poon et al. (2004d). A model for deriving the transfer functions of serially coupled ring resonators based on the time-dependent calculation as described in Sect. 2.1.1 is presented in Little et al. (1998b). Another method of simulating the transfer function of serially coupled ring resonators is by using a characteristic matrix approach presented in Chen et al. (2004a). These different methods for analyzing serially coupled ring resonators (Fig. 2.12) will be used in the following to derive the transfer functions.

The Z-transformation is used to start with in the beginning. In order to describe a serially coupled ring resonator, the filter can be broken down into two components, a symmetrical directional coupler and a pair of uncoupled guides as shown in Fig. 2.13 (Orta et al. 1995). Another way to describe the transfer function of a directional coupler is to use a chain matrix, which is given by

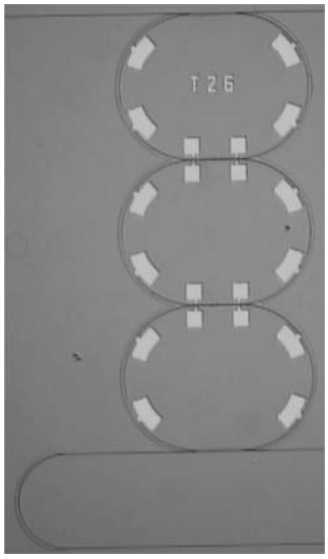

Fig. 2.12. Photograph of a serially coupled triple ring resonator

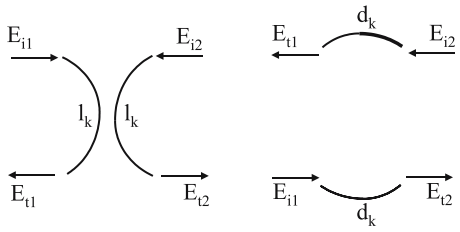

Fig. 2.13. Components of a serially coupled ring resonator filter

$$H_k^C = \mathrm{j}\mathrm{e}^{\mathrm{j}\beta l_k} \begin{bmatrix} \csc(\phi_k) & -\mathrm{e}^{-\mathrm{j}\beta l_k}\cot(\phi_k) \\ \mathrm{e}^{-\mathrm{j}\beta l_k}\cot(\phi_k) & -\mathrm{e}^{-2\mathrm{j}\beta l_k}\csc(\phi_k) \end{bmatrix}, \tag{2.104}$$

where ϕ_k is referred to as the coupling angle and l_k is the length of the coupler (note: this is not the coupling length). The chain matrix of the uncoupled guides is given by

$$H_k^R = \mathrm{e}^{\mathrm{j}\beta d_k} \begin{bmatrix} 1 & 0 \\ 0 & \mathrm{e}^{-2\mathrm{j}\beta d_k} \end{bmatrix}, \tag{2.105}$$

where d_k is the length of the ring waveguides. The chain matrix for the entire system is then expressed by

$$H = \prod_{k=N,1} \begin{bmatrix} \csc(\phi_k) & z^{-1}\mathrm{e}^{-\mathrm{j}\psi_k}\cot(\phi_k) \\ \cot(\phi_k) & z^{-1}\mathrm{e}^{-\mathrm{j}\psi_k}\csc(\phi_k) \end{bmatrix} \begin{bmatrix} \csc(\phi_0) & \cot(\phi_0) \\ \cot(\phi_0) & \csc(\phi_0) \end{bmatrix}, \tag{2.106}$$

where

$$z\mathrm{e}^{\mathrm{j}\psi_k} = -\mathrm{e}^{\mathrm{j}\beta(l_k+l_{k-1}+2d_k)}. \tag{2.107}$$

As previously described in Sect. 2.1.1 the elements of the matrix H are N degree polynomials. The chain matrix can also be compared to the chain matrix derived in (2.54). Of interest is again the transfer function for the throughput and the drop port, both related to the signal at the input port. The polynomials are given by

$$\frac{E_{t1}}{E_{i1}} = H_{11}(z) = \sum_{k=0}^{N} a_k z^{-k} \tag{2.108}$$

and

$$\frac{E_{t2}}{E_{i1}} = H_{21}(z) = \sum_{k=0}^{N} b_k z^{-k}. \tag{2.109}$$

The transfer functions of the filter are now based on the definition of these polynomials. Assuming, that the filter is lossless, the scattering matrix is unitary for $|z| = 1$. On $|z| = 1, z^* = z^{-1}$, then the relationship between (2.108) and (2.109) can be written as follows:

$$H_{11}(z)\, H_{11}^*\left(\frac{1}{z^*}\right) = 1 + H_{21}(z)\, H_{21}^*\left(\frac{1}{z^*}\right). \tag{2.110}$$

Using this equation, it is possible to calculate $H_{11}(z)$ for a given $H_{21}(z)$. The coupling angles $\phi_k\,(k = 0 \ldots N)$ and the phase shift $\psi_k\,(k = 1 \ldots N)$ are calculated as follows. First, a superscript is introduced which denotes elements belonging to the structure formed by the first $n+1$ coupler. Then the elements of the chain matrix relative to the first $(N-1)$ ring resonators, $H_{11}^{[N-1]}$ and $H_{21}^{[N-1]}$ are related to $H_{11}^{[N]}$ and $H_{21}^{[N]}$ through

$$\begin{bmatrix} \csc(\phi_N) & z^{-1}\mathrm{e}^{-\mathrm{j}\psi_N}\cot(\phi_N) \\ \cot(\phi_N) & z^{-1}\mathrm{e}^{-\mathrm{j}\psi_N}\csc(\phi_N) \end{bmatrix} \begin{bmatrix} H_{11}^{[N-1]} \\ H_{21}^{[N-1]} \end{bmatrix} = \begin{bmatrix} H_{11}^{[N]} \\ H_{21}^{[N]} \end{bmatrix}. \tag{2.111}$$

This leads to the equations for the coefficients of the polynomials (2.108) and (2.109), which are given by

$$a_k^{[N-1]} = a_k^{[N]} \csc(\phi_N) - b_k^{[N]} \cot(\phi_N) \tag{2.112}$$

and

$$b_k^{[N-1]} = \left[-a_{k+1}^{[N]} \cot(\phi_N) + b_{k+1}^{[N]} \csc(\phi_N)\right] \mathrm{e}^{\mathrm{j}\psi_N}, \tag{2.113}$$

where $k = 1 \ldots (N-1)$ and

$$a_N^{[N-1]} = b_{-1}^{[N-1]} = 0. \tag{2.114}$$

Then the coupling angle of the Nth coupler is given by

$$\cos(\phi_N) = \frac{b_0^{[N]}}{a_0^{[N]}} = \frac{a_N^{[N]}}{b_N^{[N]}}. \tag{2.115}$$

Equation (2.115) is satisfied if the ratio is real. Next step is to determine the phase shift ψ_k using (2.115) and (2.113). All other coefficients follow the same procedure.

In order to start this calculation method and derive a transfer filter characteristic, the polynomial $H_{21}^{[N]}$ has to be determined. As stated before in Sect. 2.3, a bandpass filter characteristic is preferred. When using the Z-transform, the resonant frequencies of the ring resonator filter are all placed on the circumference $|z| = 1$. For a Butterworth type filter, the "zeros" are located on $z = -1$. The zeros for a Chebyshev type of filter are given by

$$\begin{aligned} z_{0k} &= \mathrm{e}^{\left(2\mathrm{j}\arccos\left\{\sin\left(\frac{\mathrm{FWHM}}{4}\right)\cos\left(\frac{(2k-1)\pi}{2N}\right)\right\}\right)}, \\ k &= 1 \ldots N. \end{aligned} \tag{2.116}$$

This is an intuitive approach to design ring resonator filters, however it is challenging to extract the poles of the frequency response.

The time-dependent relations which have been presented for a single ring resonator can be extended to multiple serially coupled resonators. The response of the first ring (counted from the bottom of the ring filter) can be written as (Little et al. 1998b)

$$e_1 = \cfrac{-\kappa^* E_{i1}}{\mathrm{j}\Delta\omega_{\mathrm{R}1} + \cfrac{-\kappa_1^{*^2}}{\mathrm{j}\Delta\omega_{\mathrm{R}2} \ldots + \cfrac{-\kappa_{N-1}^{*^2}}{\mathrm{j}\Delta\omega_{\mathrm{R}N}}}}, \tag{2.117}$$

$$\Delta\omega_n = \left\{ \begin{array}{c} \omega - \omega_{\mathrm{R}n} - \mathrm{j}\dfrac{1}{\tau_n}, \quad n \neq 1, N \\ \omega - \omega_{\mathrm{R}n} - \mathrm{j}\dfrac{1}{\tau_n} - \mathrm{j}\dfrac{1}{\tau_{\mathrm{tr}}}, \quad n = 1, N \\ \omega - \omega_{\mathrm{R}n} - \mathrm{j}\dfrac{1}{\tau_n} - \mathrm{j}\dfrac{2}{\tau_{\mathrm{tr}}}, \quad N = 1 \end{array} \right\},$$

where ω is the optical frequency of the input wave, $\omega_{\mathrm{R}n}$ is the resonant frequency of ring resonator n and $\Delta\omega_n$ is the complex frequency deviation. The energy decay rate of each ring is given by τ_n. The response of resonator N can be expressed by a product of continued fractions:

$$e_N = E_{i1} \prod_{n=1}^{N} T_n, \tag{2.118}$$

where

$$T_N = \cfrac{-\kappa_{n-1}^*}{\mathrm{j}\Delta\omega_n + \cfrac{-\kappa_{n-1}^{*^2}}{\mathrm{j}\Delta\omega_{n-1} + \cfrac{-\kappa_{n-2}^{*^2}}{\mathrm{j}\Delta\omega_{n-2}\ldots + \cfrac{-\kappa_1^{*^2}}{\mathrm{j}\Delta\omega_{\mathrm{R1}}}}}},$$

$$T_1 = \frac{-\kappa^*}{\mathrm{j}\Delta\omega_{\mathrm{R1}}}.$$

The coefficients for maximally flat and Chebyshev filter characteristics are given in the following table for two to six serially coupled ring resonators (Little et al. 1997b):

Table 2.1. Coefficients for maximally flat and Chebyshev filter characteristics

N	maximally flat	Chebyshev
2	$\kappa_1^{*^2} = 0.250\kappa^{*4}$	$\kappa_1^{*2} = 0.250\kappa^{*2}\,(1+2y)$
3	$\kappa_1^{*2} = \kappa_2^{*2} = 0.125\kappa^{*4}$	$\kappa_1^{*2} = \kappa_2^{*2} = 0.125\kappa^{*4}\left(1+1.5y^{\frac{2}{3}}\right)$
4	$\kappa_1^{*2} = \kappa_3^{*2} = 0.100\kappa^{*4}$ $\kappa_2^{*2} = 0.040\kappa^{*4}$	
5	$\kappa_1^{*2} = \kappa_4^{*2} = 0.0955\kappa^{*4}$ $\kappa_2^{*2} = \kappa_3^{*2} = 0.040\kappa^{*4}$	
6	$\kappa_1^{*2} = \kappa_5^{*2} = 0.0915\kappa^{*4}$ $\kappa_2^{*2} = \kappa_4^{*2} = 0.0245\kappa^{*4}$ $\kappa_3^{*2} = 0.0179\kappa^{*4}$	

y determines the passband ripples of the Chebyshev filter.

Another method of calculating the transfer functions of serially coupled ring resonator filters is by using a so called characteristic matrix approach, which has been presented in Chen et al. (2004a). The method is based on defining the optical paths which an optical signal travels form the input port to the drop port. There are several paths and the shortest path is called the common path or the zeroth-order path which is defined to be unity. Looking at a serially coupled triple ring resonator, the light using the first order paths for example has three choices, one additional ring resonator path and the common path. The mth order transfer function is related to the $m+1$th order transfer function by

$$\vec{H}_{m+1} = \begin{bmatrix} H_{1,m+1} \\ H_{2,m+1} \\ H_{3,m+1} \end{bmatrix} = \begin{bmatrix} T_{11} & T_{12} & T_{13} \\ T_{21} & T_{22} & T_{23} \\ T_{31} & T_{32} & T_{33} \end{bmatrix} \cdot \begin{bmatrix} H_{1,m} \\ H_{2,m} \\ H_{3,m} \end{bmatrix} = T \cdot \vec{H}_m, \tag{2.119}$$

t_{ij} are the transfer functions of the additional path in ring resonator i, with previous path ends in ring resonator j. T is called the characteristic matrix.

Using the coefficients for the ring resonators as described previously for symmetric coupling ($t = t^*$ and $\kappa = -\kappa^*$), T is given by

$$T_{\mathrm{DropPort}} = \begin{bmatrix} t_1 t_2 \alpha_1 \mathrm{e}^{\mathrm{j}\theta_1} \left(1 \ \frac{-\kappa_2^2}{t_2^2} \ 0\right) \\ t_2 t_3 \alpha_2 \mathrm{e}^{\mathrm{j}\theta_2} \left(1 \ 1 \ \frac{-\kappa_3^2}{t_3^2}\right) \\ t_3 t_4 \alpha_3 \mathrm{e}^{\mathrm{j}\theta_3} \left(1 \ 1 \ 1\right) \end{bmatrix}. \tag{2.120}$$

The general expression for the characteristic matrix for a filter consisting of n ring resonators is given by

$$T_{\mathrm{DropPort}} = \begin{bmatrix} t_1 t_2 \alpha_1 \mathrm{e}^{\mathrm{j}\theta_1} \left(1 \ \frac{-\kappa_2^2}{t_2^2} \ 0 \ldots 0\right) \\ t_2 t_3 \alpha_2 \mathrm{e}^{\mathrm{j}\theta_2} \left(1 \ 1 \ \frac{-\kappa_3^2}{t_3^2} \ 0 \ldots 0\right) \\ \ldots \left(1 \ldots 1 \ldots 0\right) \\ \ldots \left(1 \ldots \ldots 1 \ \frac{-\kappa_n^2}{t_n^2}\right) \\ t_n t_{n+1} \alpha_n \mathrm{e}^{\mathrm{j}\theta_n} \left(1 \ldots \ldots 1 \ 1\right) \end{bmatrix}. \tag{2.121}$$

The general expression for the transfer function for the drop port is then given by

$$H_{\mathrm{DropPort}} = \frac{\prod_k \kappa_k \sqrt{\prod_k \alpha_k} \mathrm{e}^{\mathrm{j}\sum_k \theta_k}}{|U_{Matrix} - T_{\mathrm{DropPort}}|}, \quad k = 1 \ldots n, \tag{2.122}$$

where U_{Matrix} is the unit matrix.

Filter synthesis using (2.121) and (2.122) can be done by solving a matrix eigenvalues equation. The poles of a filter function correspond to unity minus the eigenvalues of T_{DropPort}. The eigenvalues and power coupling ratios for a maximally flat transfer function are given in Table 2.2 assuming lossless devices.

Using the aforementioned techniques, it is possible to find the transfer functions for arbitrary serially coupled ring resonators. Each method has its pros and cons and therefore it is left to the designer to choose the right method which seems convenient to solve the problem. When designing ring resonator filters, it is appropriate to evaluate the technological feasibility of certain parameters like coupling coefficients and loss in order to easily transfer the design to fabrication.

A special serially coupled ring resonator design (Fig. 2.14) has been proposed and analyzed in Poon, Scheuer, Yariv (2004e). The following calculation method is based on this literature.

Table 2.2. Eigenvalues and power coupling ratios for a maximally flat transfer function

N	eigenvalues (= 1 – poles)	power coupling ratios
2	$0.63 + 0.32\mathrm{i};\ 0.63 - 0.32\mathrm{i}$	0.5; 0.2; 0.5
3	$0.73 + 0.42;\ 0.71;\ 0.73 - 0.42\mathrm{i}$	0.5; 0.14; 0.14; 0.5
4	$0.78 + 0.45\mathrm{i};\ 0.77 + 0.17\mathrm{i};\ 0.77 - 0.17\mathrm{i};$ $0.78 - 0.45\mathrm{i}$	0.5; 0.13; 0.09; 0.13; 0.5
5	$0.81 + 0.46\mathrm{i};\ 0.8 + 0.26\mathrm{i};\ 0.81;\ 0.8 -$ $0.26\mathrm{i};\ 0.81 - 0.46\mathrm{i}$	0.5; 0.13; 0.08; 0.08; 0.13; 0.5
10	$0.86 + 0.48\mathrm{i};\ 0.85 + 0.42\mathrm{i};\ 0.86 + 0.33\mathrm{i};$ $0.88 + 0.21\mathrm{i};\ 0.9 + 0.07\mathrm{i};\ 0.9 - 0.07\mathrm{i};$ $0.88 - 0.21\mathrm{i};\ 0.86 - 0.33\mathrm{i};\ 0.85 - 0.42\mathrm{i};$ $0.86 - 0.48\mathrm{i}$	0.5; 0.12; 0.07; 0.07; 0.07; 0.07; 0.07; 0.07; 0.07; 0.12; 0.5

(Chen et al. 2004a)

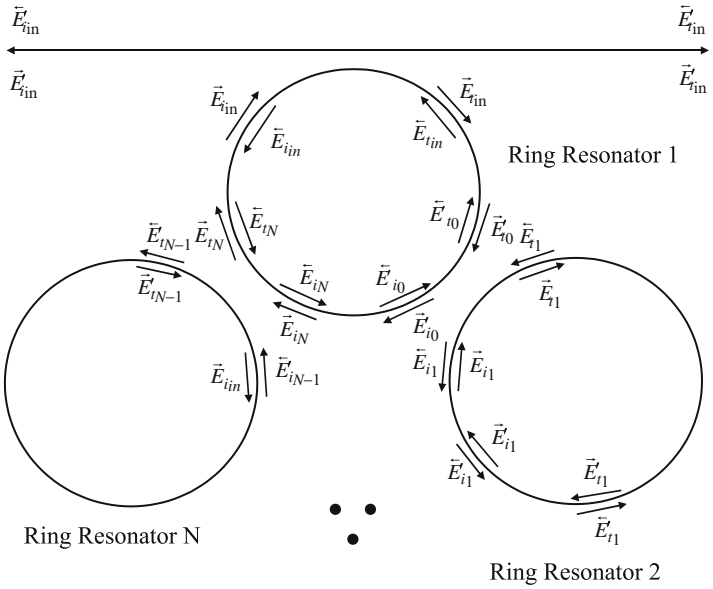

Fig. 2.14. Ring resonator configuration with interring coupling

Depending on the number of rings used the filter can either be reflecting or nonreflecting. The filter acts as a reflector for an odd number of rings (N $\geq$ 3), whereas a nonreflecting filter is obtained for an even number of rings (N $\geq$ 4). The transfer functions are derived by using a transfer matrix method, starting in defining a vector x_n, which represents the field component in ring resonator $n-1$:

$$x_n = \left[\overleftarrow{E}_\mathrm{t}\ \overleftarrow{E}_i\ \overrightarrow{E}_i\ \overrightarrow{E}_\mathrm{t}\right]_n^\mathrm{T} \tag{2.123}$$

The arrows used as superscripts are as described earlier for the double ring the direction of the propagating field, clockwise or anticlockwise without mixing of waves between the two directions. The coupling between the ring resonators can be represented by the following 4×4 matrix ($n \geq 0$):

$$x_{n+1} = \begin{bmatrix} \frac{-t}{\kappa} & \frac{1}{\kappa} & 0 & 0 \\ -\frac{1}{\kappa} & \frac{t^*}{\kappa} & 0 & 0 \\ 0 & 0 & \frac{-t}{\kappa} & \frac{1}{\kappa} \\ 0 & 0 & -\frac{1}{\kappa} & \frac{t^*}{\kappa} \end{bmatrix} \cdot x'_n = M_{\mathrm{P}} \cdot x'_n. \tag{2.124}$$

Assuming only the phase matched waves are being coupled ($L_{Coupler} \gg \lambda$).

The vector x'_n is related to x_n by the following propagation matrix:

$$x'_n = \begin{bmatrix} 0 & 0 & 0 & \mathrm{e}^{-\mathrm{j}\beta r\theta} \\ 0 & 0 & \mathrm{e}^{\mathrm{j}\beta r(2\pi-\theta)} & 0 \\ 0 & \mathrm{e}^{\mathrm{j}\beta r(2\pi-\theta)} & 0 & 0 \\ \mathrm{e}^{-\mathrm{j}\beta r\theta} & 0 & 0 & 0 \end{bmatrix} \cdot x_n = M_Q \cdot x_n, \tag{2.125}$$

$$\theta = 2\pi - \frac{\pi\,(N-2)}{N}.$$

Combining (2.124) and (2.125)

$$x_{n+1} = M_{\mathrm{P}} \cdot x'_n = M_{\mathrm{P}} \cdot M_{\mathrm{Q}} \cdot x_n = M_{\mathrm{T}} \cdot x_n. \tag{2.126}$$

For an N type ring resonator configuration with $N > 2$, (2.126) yields:

$$x_N = {M_{\mathrm{T}}}^{N-1} \cdot M_{\mathrm{P}} \cdot x'_0 = M_{\mathrm{A}} \cdot x'_0. \tag{2.127}$$

Only the components of vector x'_{in} hold the transfer functions, therefore the transfer functions of the ring resonator configuration are derived using the relation for the coupling to the external waveguide and the phase relations in the first resonator:

$$x_{\mathrm{in}} = M_{P_{\mathrm{in}}} \cdot x'_{\mathrm{in}}, \tag{2.128}$$

$$\begin{aligned} \overrightarrow{E}_{t0} &= \overrightarrow{E}_{t_{\mathrm{in}}} \mathrm{e}^{-\mathrm{j}\beta r\frac{\theta}{2}} & \overleftarrow{E'}_{t0} &= \overleftarrow{E}_{t_{\mathrm{in}}} \mathrm{e}^{\mathrm{j}\beta r\frac{\theta}{2}}, \\ \overrightarrow{E'}_{i0} &= \overrightarrow{E}_{iN} \mathrm{e}^{\mathrm{j}\beta r(2\pi-\theta)} & \overleftarrow{E'}_{i0} &= \overleftarrow{E}_{iN} \mathrm{e}^{-\mathrm{j}\beta r(2\pi-\theta)}, \\ \overleftarrow{E}_{tN} &= \overleftarrow{E}_{i_{\mathrm{in}}} \mathrm{e}^{-\mathrm{j}\beta r\frac{\theta}{2}} & \overrightarrow{E}_{tN} &= \overrightarrow{E}_{i_{\mathrm{in}}} \mathrm{e}^{\mathrm{j}\beta r\frac{\theta}{2}}. \end{aligned}$$

Using (2.127) and (2.128), x_N and x'_0 can be expressed by elements of x_{in}. Equation (2.127) can then be rewritten as

$$\begin{aligned} m M_{P_{\mathrm{in}}} x'_{\mathrm{in}} &= M_{\mathrm{T}}^{N-1} M_{\mathrm{P}} w M_{\mathrm{Pin}} x'_{\mathrm{in}} \\ \Rightarrow x'_{\mathrm{in}} &= M_{\mathrm{B}} x'_{\mathrm{in}}, \end{aligned} \tag{2.129}$$

where m and w represent matrices which express the terms $\overleftarrow{E}_{i_n}$, $\overrightarrow{E}_{i_n}$ and $\overrightarrow{E'_{i0}}$, $\overrightarrow{E'_{i0}}$, using components of vector x_{in} respectively. The matrix M_{B} can then be expressed by

$$M_{\mathrm{B}} = M_{\mathrm{Pin}}^{-1} m^{-1} M_{\mathrm{T}}^{N-1} M_{\mathrm{P}} w M_{\mathrm{Pin}}. \tag{2.130}$$

If only one input is considered as in the previous ring resonator examples, x'_{in} can be expressed by

$$x'_{\mathrm{in}} = \left[0 \ \overrightarrow{E'_{i_{\mathrm{in}}}} \ 1 \ \overleftarrow{E'_{t_{\mathrm{in}}}}\right]^{\mathrm{T}}. \tag{2.131}$$

The reflection and transmission function $\overrightarrow{E'_{i_{\mathrm{in}}}}$ and $\overrightarrow{E'_{t_{\mathrm{in}}}}$ can then be derived using elements of matrix M_{B} and solving the following matrix equation:

$$\begin{bmatrix} \dfrac{M_{B_{4,2}}}{1 - M_{\mathrm{B}_{4,4}}} & 1 \\ 1 & -\dfrac{M_{\mathrm{B}_{2,4}}}{1 - M_{\mathrm{B}_{2,2}}} \end{bmatrix} \begin{bmatrix} \overrightarrow{E'}_{i_{\mathrm{in}}} \\ \overleftarrow{E'}_{t_{\mathrm{in}}} \end{bmatrix} = \begin{bmatrix} \dfrac{M_{\mathrm{B}_{4,3}}}{1 - M_{\mathrm{B}_{4,4}}} \\ \dfrac{M_{\mathrm{B}_{2,3}}}{1 - M_{\mathrm{B}_{2,2}}} \end{bmatrix}. \tag{2.132}$$

The following equations are also valid for the solutions:

$$\begin{aligned} M_{\mathrm{B}_{3,2}} \overrightarrow{E'}_{i_{\mathrm{in}}} + M_{\mathrm{B}_{3,3}} + M_{\mathrm{B}_{3,4}} \overleftarrow{E'}_{t_{\mathrm{in}}} &= 1, \\ M_{\mathrm{B}_{1,2}} \overrightarrow{E'}_{i_{\mathrm{in}}} + M_{\mathrm{B}_{1,3}} + M_{\mathrm{B}_{1,4}} \overleftarrow{E'}_{t_{\mathrm{in}}} &= 0. \end{aligned} \tag{2.133}$$

In using the above equations, it is possible to calculate the reflectance and the transmittance spectra of this type of serially interring coupled ring resonator.

2.3.2 Parallel Coupled Ring Resonators

Parallel coupled ring resonators have been addressed in literature and the transfer functions have been derived by several methods. One of the advantages of parallel coupled ring resonators over serially coupled ring resonators is that their transfer functions are less sensitive to fabrication tolerances, as each ring resonator can compensate errors in any of the others. Two configurations are discussed, one where the ring resonators are coupled to two input/output waveguides and the other, where all share one input/output waveguide.

Coupled to Two Input/Output Waveguides

As can be seen from Fig. 2.15, parallel coupled ring resonators coupled to two waveguides share the same input, throughput, drop, and add port.

The synthesis of the transfer functions of parallel coupled ring resonators using a recursive algorithm is presented in Little et al. (2000a). A complex matrix formalism employing racetrack ring resonator filters is derived in Griffel (2000a). A technique using simple closed-form formulas to determine

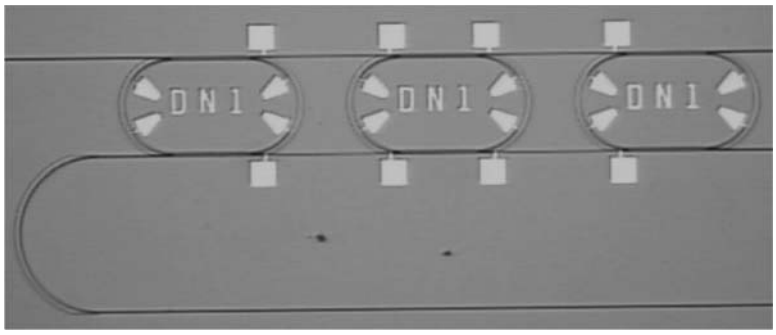

Fig. 2.15. Photograph of a parallel coupled triple ring resonator

the Q factor of each involved ring resonator which leads to the coupling coefficients is demonstrated in Melloni (2001). These different methods for analyzing the transfer functions will be used in the following.

The model which has been presented in Fig. 2.10 can be easily extended for multiple parallel coupled ring resonators. The distance between the uncoupled ring resonators Λ is chosen so that the transfer functions of each ring resonator add in phase. The transfer function derived by the recursive algorithm used in Little et al. (2000a) is given by

$$T_n = \frac{E_\mathrm{t}}{E_i} = R_n - \frac{E^i_{\mathrm{t}\,n} E^o_{\mathrm{t}\,n}}{R_n - T^{-1}_{n-1} \mathrm{e}^{\mathrm{j}2\theta_{\mathrm{W}\,n-1}}}, \tag{2.134}$$

$$R_n = -\frac{\mu^i_n \mu^o_n}{\mathrm{j}\Delta\omega + \frac{1}{2}\left(\mu^{i,o}_n\right)^2 + \frac{1}{2}\left(\mu^{i,o}_n\right)^2},$$

$$E^{i,o}_{\mathrm{t}\,n} = R_n - \frac{\left(\mu^{i,o}_n\right)^2}{\mathrm{j}\Delta\omega + \frac{1}{2}\left(\mu^{i,o}_n\right)^2 + \frac{1}{2}\left(\mu^{i,o}_n\right)^2},$$

where the indices i, o correspond to the through responses of each ring resonator n in the waveguides joining the ring resonators and $\Delta\omega$ is the frequency deviation away from resonance. The term μ is related to the coupling coefficient κ (2.74):

$$\mu^{i,o}_n = \kappa^{i,o}_n \sqrt{\frac{v_{\mathrm{g}\,n}}{2\pi r_n}}. \tag{2.135}$$

The recursion is started with $T_1 = R_1$. Loss can also be incorporated into this algorithm by substituting $\mathrm{j}\Delta\omega$ with $\mathrm{j}\Delta\omega + 1/\tau$.

In this type of synthesis, the transfer function is directly related to the coupling coefficient to obtain any desired filter shape. In the methods described earlier, the transfer functions are rational polynomials related to frequency, wavelength or z where the coefficients of the polynomials are adjusted for any specific filter function. In using the recursive algorithm, it is possible to

suppress unwanted sidelobes by apodization, which is realized by adjusting the coupling coefficients properly.

A straight forward method of designing parallel coupled ring resonator filters is presented in Melloni (2001). The filter shape can be calculated by using the given specifications for bandwidth, FSR, out of band rejection and selectivity. The formulas for a parallel N coupled ring resonator filter are as follows:

$$Q_n = \frac{\mathrm{FSR}}{g_n FWHM} \tag{2.136}$$
$$g_n = \sqrt{2}\sin\left(\frac{2n-1}{2N}\pi\right).$$

The coupling coefficients are given by

$$\kappa_n = \frac{\pi^2}{2{Q_n}^2}\left[\sqrt{1+\frac{4{Q_n}^2}{\pi^2}}-1\right]. \tag{2.137}$$

A specific filter characteristic can be derived by using this method and the relations described in Sect. 2.1.1.

For deriving the transfer functions for parallel coupled racetrack shaped ring resonators, the matrix formalism described in Griffel (2000a) is used. The parallel coupled filter can be broken down into two components, similar to the method shown for the serially coupled ring resonator filter, into a ring resonator coupled to two waveguides and into a pair of uncoupled guides as shown in Fig. 2.16.

The transfer matrix for the ring resonator coupled to two waveguides is given by

$$\begin{pmatrix} \overleftarrow{E}_i \\ \overrightarrow{E}_i \\ \overleftarrow{E}_t \\ \overrightarrow{E}_t \end{pmatrix}_n = \begin{pmatrix} \frac{a_{1_n}a_{2_n}-b_n^2}{a_{2_n}} & 0 & 0 & -\frac{b_n}{a_{2_n}} \\ 0 & \frac{1}{a_{1_n}} & \frac{b_n}{a_{1_n}} & 0 \\ 0 & -\frac{b_n}{a_{1_n}} & \frac{a_{1_n}a_{2_n}-b_n^2}{a_{1_n}} & 0 \\ \frac{b_n}{a_{2_n}} & 0 & 0 & \frac{1}{a_{2_n}} \end{pmatrix} \cdot \begin{pmatrix} \overleftarrow{E}_i \\ \overrightarrow{E}_i \\ \overleftarrow{E}_t \\ \overrightarrow{E}_t \end{pmatrix}_{n+1}. \tag{2.138}$$

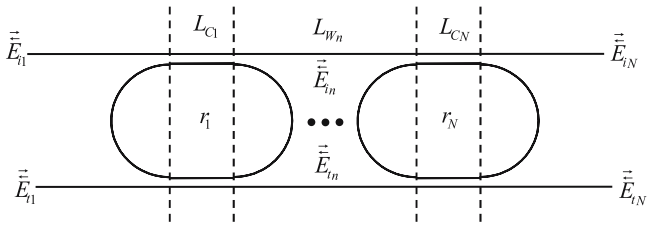

Fig. 2.16. Schematic of a parallel coupled ring resonator filter

The transfer matrix for the pair of uncoupled waveguides is given by

$$\begin{pmatrix} \overleftarrow{E}_i \\ \overrightarrow{E}_i \\ \overleftarrow{E}_t \\ \overrightarrow{E}_t \end{pmatrix}_n = \begin{pmatrix} \mathrm{e}^{\mathrm{j}\beta_W L_{\mathrm{W}n}} & 0 & 0 & 0 \\ 0 & \mathrm{e}^{-\mathrm{j}\beta_W L_{\mathrm{W}n}} & 0 & 0 \\ 0 & 0 & \mathrm{e}^{\mathrm{j}\beta_W L_{\mathrm{W}n}} & 0 \\ 0 & 0 & 0 & \mathrm{e}^{-\mathrm{j}\beta_W L_{\mathrm{W}n}} \end{pmatrix} \cdot \begin{pmatrix} \overleftarrow{E}_i \\ \overrightarrow{E}_i \\ \overleftarrow{E}_t \\ \overrightarrow{E}_t \end{pmatrix}_{n+1} . \tag{2.139}$$

The coefficients a_{1n}, a_{2n} and b_n are given by

$$\begin{aligned} b_n &= \frac{\kappa_{1_n}\kappa_{2_n}\mathrm{e}^{-\mathrm{j}(2\beta_W L_{\mathrm{C}n}+\beta_{\mathrm{R}}\pi r_n)}}{1-t_{1_n}t_{2_n}\mathrm{e}^{-2\mathrm{j}(\beta_W L_{C_n}+\beta_{\mathrm{R}}\pi r_n)}}, \\ a_{1_n} &= \frac{t_{2_n}\mathrm{e}^{-\mathrm{j}\beta_W L_{\mathrm{C}n}} - t_{1_n}\mathrm{e}^{-\mathrm{j}(3\beta_W L_{\mathrm{C}n}+2\beta_{\mathrm{R}}\pi r_n)}}{1-t_{1_n}t_{2_n}\mathrm{e}^{-2\mathrm{j}(\beta_W L_{\mathrm{C}n}+\beta_{\mathrm{R}}\pi r_n)}}, \\ a_{2_n} &= \frac{t_{1_n}\mathrm{e}^{-\mathrm{j}\beta_W L_{\mathrm{C}n}} - t_{2_n}\mathrm{e}^{-\mathrm{j}(3\beta_W L_{\mathrm{C}n}+2\beta_{\mathrm{R}}\pi r_n)}}{1-t_{1_n}t_{2_n}\mathrm{e}^{-2\mathrm{j}(\beta_W L_{\mathrm{C}n}+\beta_{\mathrm{R}}\pi r_n)}}. \end{aligned} \tag{2.140}$$

The arrows used as the superscripts indicate whether the field is propagating to the left or the right direction. Multiplying the transfer matrices in an alternating rhythm, the transfer functions for a parallel N coupled ring resonator filter can be derived. Note that in the calculation the propagation constant for the uncoupled waveguides and for the ring resonators is assumed to be the same for each one, respectively. The drop port $\overleftarrow{E}_{t1}$ and the throughput $\overrightarrow{E}_{iN}$ responses from the resulting matrix H, where h represent the elements of the matrix, are then given by (assuming only one input, $\overrightarrow{E}_{i1} = 1$):

$$\begin{aligned} &\overleftarrow{E}_{t1} = \frac{h_{3,2}}{h_{2,2}} \quad \overrightarrow{E}_{iN} = \frac{1}{h_{2,2}}, \\ &\text{where} \quad \overrightarrow{E}_{tN} = \overleftarrow{E}_{i1} = 0. \end{aligned} \tag{2.141}$$

As in the recursive algorithm mentioned earlier in this chapter, the coupling coefficients can also be varied to control the bandwidth of the filter and thus reducing the sidelobes by apodization.

Several configurations to obtain a box-like filter response using an array of parallel coupled ring resonators are presented in Ma et al. (2005). A special configuration consisting of a parallel coupled double ring resonator (with two waveguides), serially coupled with a single ring resonator has been analyzed in Okamoto et al. (2003).

Coupled to One Input/Output Waveguide

The basic ring resonator filter configuration consisting of a ring and a waveguide is used to realize a multiple parallel coupled filter. Another term for

parallel coupled ring resonators with only one input/output waveguides is side-coupled, integrated, space sequence of resonators (SCISSORS) (Heebner et al. 2002). The transfer functions of these types of filters can be derived using the methods and formulas described earlier in this chapter. In this chapter the focus lies on the optical properties of this kind of device which have been analyzed in detail in Heebner et al. (2002) and Pereira et al. (2002). The following expressions are based on this literature.

In order to describe linear propagation effects, a pulse is considered, which travels through a single ring resonator, obtaining a frequency-dependent phase shift that results in a delay or distorts the pulse shape (see also section "The Time-Dependent Relations"). The effective propagation constant for a resonator spacing of Λ is then given by

$$\beta_0(\omega) = \frac{n_{\text{eff}}\omega}{c_0} + \frac{\Phi(\omega)}{\Lambda}, \tag{2.142}$$

where $\Phi(\omega)$ is the phase shift which a field acquires when traversing a ring resonator. It is derived from the transfer function of a single ring resonator (Fig. 2.2) where the throughput field is related to the input field (2.9).

$$\begin{aligned} E_{t1}(\omega) &= \mathrm{e}^{\mathrm{j}\Phi(\omega)} E_{i1}(\omega), \\ \Phi(\omega) &= \pi + \theta(\omega) + 2\arctan\left(\frac{t\sin\theta(\omega)}{1 - t\cos\theta(\omega)}\right). \end{aligned} \tag{2.143}$$

The transfer function of a single ring resonator can be expanded into two terms using the Taylor series, representing the transmitted (expanded about the normalized detuning θ_0) and the exponential phase shift (expanded about the transmitted phase shift of the carrier Φ_0). The transfer function is given by

$$H(\omega) = \mathrm{e}^{\mathrm{j}\Phi} = \mathrm{e}^{\mathrm{j}\Phi_0}\left\{1 + \sum_{n=1}^{\infty}\frac{j^n}{n!}\left[\sum_{m=1}^{\infty}\frac{1}{m!}\left.\frac{\mathrm{d}^m\Phi}{\mathrm{d}\theta^m}\right|_{\theta_0} \times (\theta - \theta_0)^m\right]^n\right\}. \tag{2.144}$$

Using this equation, the field at some point z_{l+1} expressed by the field at another point z_l which is only a small distance δz away is given by (the transmitted phase shift induced by each ring resonator is assumed to be distributed over the separation Λ, leading to an effective propagation constant which is independent of propagation distance):

$$\begin{aligned} E_{l+1}(\omega) = \exp\left[\mathrm{j}\left(\frac{n_{\text{eff}}\omega_0}{c_0} + \frac{\Phi_0}{\Lambda}\right)\delta z\right] \\ \times\left\{1 + \sum_{n=1}^{\infty}\frac{j^n}{n!}\left[\frac{n_{\text{eff}}}{c_0}\Delta\omega\delta z + \sum_{m=1}^{\infty}\frac{1}{m!}\frac{\delta z}{\Lambda}\left.\frac{\mathrm{d}^m\Phi}{\mathrm{d}\theta^m}\right|_{\theta_0}(\theta - \theta_0)^m\right]^n\right\} E_l(\omega). \end{aligned} \tag{2.145}$$

The Fourier transform of (2.145) leads to a difference equation for the transfer function expanded to two Tailor series (transmitted and exponential phase shift)

$$A_{l+1}(t) = A_l(t) + \sum_{n=1}^{\infty} \frac{j^n}{n!} \left[\mathrm{j} \frac{n_{\mathrm{eff}}}{c_0} \delta z \frac{\partial}{\partial t} + \sum_{m=1}^{\infty} \frac{1}{m!} \frac{\delta z}{\Lambda} \frac{\mathrm{d}^m \Phi}{\mathrm{d}\omega^m}\bigg|_{\theta_0} \left(\frac{j}{\mathrm{FSR}} \frac{\partial}{\partial t} \right)^m \right]^n A_l(t) \tag{2.146}$$

For weak coupling, (2.146) can be rewritten using

$$\frac{A_{l+1}(t) - A_l(t)}{\delta z} \xrightarrow{\delta z \to 0} \frac{\mathrm{d}A}{\mathrm{d}z} \tag{2.147}$$

leading to

$$\frac{\mathrm{d}A}{\mathrm{d}z} = \left[-\frac{n_{\mathrm{eff}}}{c_0} \frac{\partial}{\partial t} + \mathrm{j} \sum_{m=1}^{\infty} \frac{1}{m!} \frac{1}{\Lambda} \frac{\mathrm{d}^m \Phi}{\omega^m}\bigg|_{\theta_0} \left(\frac{j}{\mathrm{FSR}} \frac{\partial}{\partial t} \right)^m \right] A. \tag{2.148}$$

This equation yields the group-velocity reduction and group-velocity dispersion including higher order dispersion. The group-velocity reduction, which is proportional to the inverse of the first frequency derivative of the propagation constant, is given by the term:

$$\beta'_{\mathrm{eff}} = \frac{\mathrm{d}\beta_{\mathrm{eff}}}{\mathrm{d}\omega} = \frac{n_{\mathrm{eff}}}{c_0} + \frac{1}{\Lambda} \frac{\mathrm{d}\Phi}{\mathrm{d}\omega} \xrightarrow{\theta_0 = 0, t \approx 1} \frac{n_{\mathrm{eff}}}{c_0} \left(1 + \frac{4r}{\Lambda} F \right), \tag{2.149}$$

where F is the finesse and r the radius of the ring resonator (see (2.30)). The group-velocity dispersion, which is proportional to the second frequency derivative of the effective propagation constant, is given by:

$$\beta''_{\mathrm{eff}} = \frac{\mathrm{d}\beta^2_{\mathrm{eff}}}{\mathrm{d}\omega^2} = \frac{1}{\Lambda} \frac{\mathrm{d}^2 \Phi}{\mathrm{d}\omega^2} \xrightarrow{\theta_0 = \pm \frac{\pi}{F\sqrt{3}}} \mp \frac{3\sqrt{3} F^2}{4\pi^2 \Lambda \mathrm{FSR}^2}. \tag{2.150}$$

The dispersion maxima are obtained at a detuning of $\theta_0 = \pm \frac{\pi}{F\sqrt{3}}$.

Higher-order dispersion is derived in a similar way as described before. The expression for the third-order dispersion is given by the term:

$$\beta'''_{\mathrm{eff}} = \frac{1}{\Lambda} \frac{\mathrm{d}^3 \Phi}{\mathrm{d}\omega^3}, \xrightarrow{\theta_0 = 0, t \approx 1} -\frac{4}{\pi^3} \frac{F^3}{\Lambda \mathrm{FSR}^3}. \tag{2.151}$$

All orders of dispersion have to be taken into account if the pulse bandwidth corresponds approximately to the resonance bandwidth given by the FWHM.

Ring resonators are versatile devices and do not only exhibit linear properties, but can also be used to realize nonlinear effects. This can be accomplished by using a material system like InGaAsP or GaAs for example. The effective nonlinear propagation constant is given by (assuming that the nonlinearity of the bus waveguide does not contribute significantly and can be neglected):

$$\beta^{nl}{}_{\mathrm{eff}} = \frac{1}{\Lambda} \frac{\mathrm{d}\Phi}{\mathrm{d}\left|E_{i1}\right|^2} = \frac{1}{\Lambda} \frac{\mathrm{d}\Phi}{\mathrm{d}\theta} \frac{\mathrm{d}\theta}{\mathrm{d}\left|E_{i2}\right|^2} \frac{\mathrm{d}\left|E_{i2}\right|^2}{\mathrm{d}\left|E_{i1}\right|^2} \xrightarrow{\theta_0 = 0, t \approx 1} \beta^{nl} \frac{8r}{\pi \Lambda} F^2. \tag{2.152}$$

The linear propagation (2.148) can then be modified to:

$$\frac{\mathrm{d}A}{\mathrm{d}z} = \left[-\frac{n_{\mathrm{eff}}}{c_0}\frac{\partial}{\partial t} + \mathrm{j}\sum_{m=1}^{\infty}\frac{1}{m!}\frac{1}{\Lambda}\frac{\mathrm{d}^m \Phi}{\omega^m}\bigg|_{\theta_0} \times \left(\beta^{nl} 2\pi r B\left|A\right|^2 + \frac{j}{FSR}\frac{\partial}{\partial t}\right)^m \right] A, \tag{2.153}$$

where B is the intensity enhancement or buildup factor (see (2.32)–(2.36)).

This configuration of side-coupled ring resonators exhibits strong dispersive and nonlinear properties and also supports solitons. As fabrication technologies mature, integration of these kinds of devices becomes feasible.

The following chapter highlights the realization and characterization of ring resonator devices in different material systems.

http://www.springer.com/978-3-540-68786-3

Integrated Ring Resonators
The Compendium
Rabus, D.G.
2007, XVI, 258 p. 243 illus., Hardcover
ISBN: 978-3-540-68786-3